Original Article

Geology and geochemistry of the only independent tellurium deposit in the world

Jianzhao Yin[1] ©, Haoyu Yin[2], Yuhong Chao[3], Shoupu Xiang[4], and Hongyun Shi[1]

Abstract

The article discusses both the regional and deposit geology including structure, strata, and igneous rocks, as well as the ore body and alteration of Dashuigou tellurium deposit at the Qinghai-Tibet Plateau, the only independent tellurium deposit in the world. There are over 30 minerals that make up the deposit's ore, including carbonates, silicates, oxides, sulfides including various tellurides and native element minerals. Euhedral, semi-euhedral, xenomorphic granular, metasomatic, metasomatic graphic, reaction rim, and solid solution separation are the main ore texture; while massive, vein/veinlet, stockwork, dissemination, breccia, and bird's-eye are the major ore structure of the deposit. Based on the ore structure, this deposit's ore can be divided into three categories: massive, veinlet-stockwork, and disseminated. The ores are further divided into eight subcategories in total based on the proportions of tellurium minerals, other sulfides, dolomite, quartz, and muscovite in it. Both geology and K-Ar isotope dating have confirmed that the pyritic (pyrrhotite + pyrite) vein and telluride vein are products of two different geological events that are far apart. The tellurium grade in the ores varies between 0.01% and 34.58%. All ores in this deposit are primary sulfide ores that have not been transformed by oxidation or weathering. Two paragenetic stages; namely, the pyritic stage and tellurium stage consisting of five sub-stages in total exist in the deposit. According to Laznicka's idea, the deposit's tonnage accumulation indices indicate that it is a super-large independent tellurium deposit.

Key words: geology; geochemistry; ore; tonnage accumulation index; independent tellurium deposit; Qinghai-Tibet Plateau

---

Affiliation Info: [1] Orient Resources Ltd., Richmond, British Columbia, V7E 1M8, Canada; [2] Guinea Westfield Mining Company-Sarlu, Jinzhong 031300, China; [3] Ganzhongnan Institute of Geology and Mineral Exploration, Nanchang 330002, China; [4] Silvercorp Metals Inc., Beijing 100027, China

Article Info: Received: 18 August 2023 / Revised: 30 October 2023 / Accepted: 16 November 2023 / Published Online: 12 December 2023. www.naturalisscientias.com

Authors' Contact Info: Yin, JZ: jimyin7@yahoo.ca; Yin, HY: yinhaoyu11@163.com; Chao, YH: 435975944@qq.com; Xiang, SP: shoupux@163.com; Shi, HY: hongyunshi@yahoo.com

Citation: Yin, JZ; Yin, HY; Chao, YH; Xiang, SP and Shi, HY. 2024. Geology and geochemistry of the only independent tellurium deposit in the world. *Naturalis Scientias*, 1(1): 1-31. DOI: https://doi.org/10.62252/NSS.2024.1001.

Corresponding Author©: Yin, JZ, PhD, PGeo, Professor; Email: jimyin7@yahoo.ca

1 Introduction

As one of the scattered elements that have similar geochemical characteristics with Clark values too low to enrich into independent deposits, tellurium (Te) was usually thought to exist only as associated components in other metallic deposits and not to form independent deposits in the traditional theory of mineral deposits. According to Li[1-3], the average content of Te in the Earth's crust is 2.0×10^{-8} in China, and 1.34×10^{-9} worldwide.
As a fact, the world's supply of refined tellurium is mainly recovered from Te-bearing ores including chalcopyrite, pyrite, pyrrhotite, volcanogenetic sulfur, bismuthinite, gold, silver, arsenopyrite, and cassiterite deposits, and most of the recoverable Te in the world is from copper deposits[4-6].
As the only independent tellurium deposit in the world thus far, the Dashuigou tellurium deposit, which is located in Simian county, Sichuan Province, China (Fig. 1)[7], has aroused widespread concern from geologists, since its discovery in 1992[8-27].

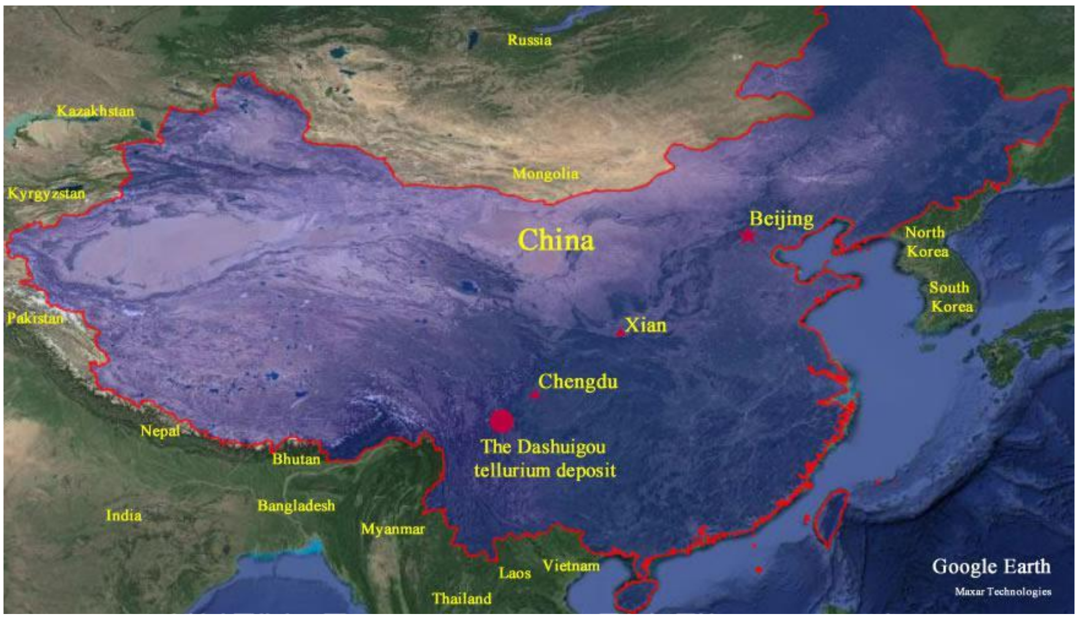

Figure 1. Location map (after Yin & Shi 2020a)[7]

(Google Earth 7.1.8.3036 (32-bit): http://download.pchome.net/industry/geography/detail-20351.html, and 91 v17.5.8: www.91weitu.com; accessed January 25-27, 2020)

Putting aside the many different views on the origin of this deposit, this article discusses in detail the deposit's geology and geochemistry. The genesis and origin are left to the relevant readers to think and discuss.

2 Regional geology

2.1 Geotectonic background

Nestled in the convergence between the Indian, Eurasian, and Pacific Plates, the Dashuigou tellurium deposit is located in the transitional belt between the Yangtze paraplatform and Songpan-Ganzi folded belt, as part of the Qinghai - Tibet Plateau (Fig. 2)[4 & 28-29].

According to the previous researches[4,16-18 & 28-31], the area has the following geophysical characteristics: high geothermal flow, high velocity, high density, high resistance, and high magnetism; a turning boundary of the Earth's crust's thickness: from the 31-40 km thickness of the South China block, through the 50-55 km thickness of this area, to the 60-75 km thickness of the Qinghai-Tibet Plateau; a gravity gradient zone which controls both the production and development of earthquakes and tectonomagmatic events, and the distribution of a series of mineral deposits; upper mantle below the region uplifting obviously. There is also a low-velocity and low resistivity zone in the middle crust that is interpreted as a decollement. The abnormal mantle exists under the crust in the region, which has properties of geosyncline and platform, as well as its own special characteristics. The belt is a geo-tectonically active zone with very complicated igneous rock structures.

In summary, this region is both geologically very active and a very important south-north trending tectonomagmatic-mineral belt.

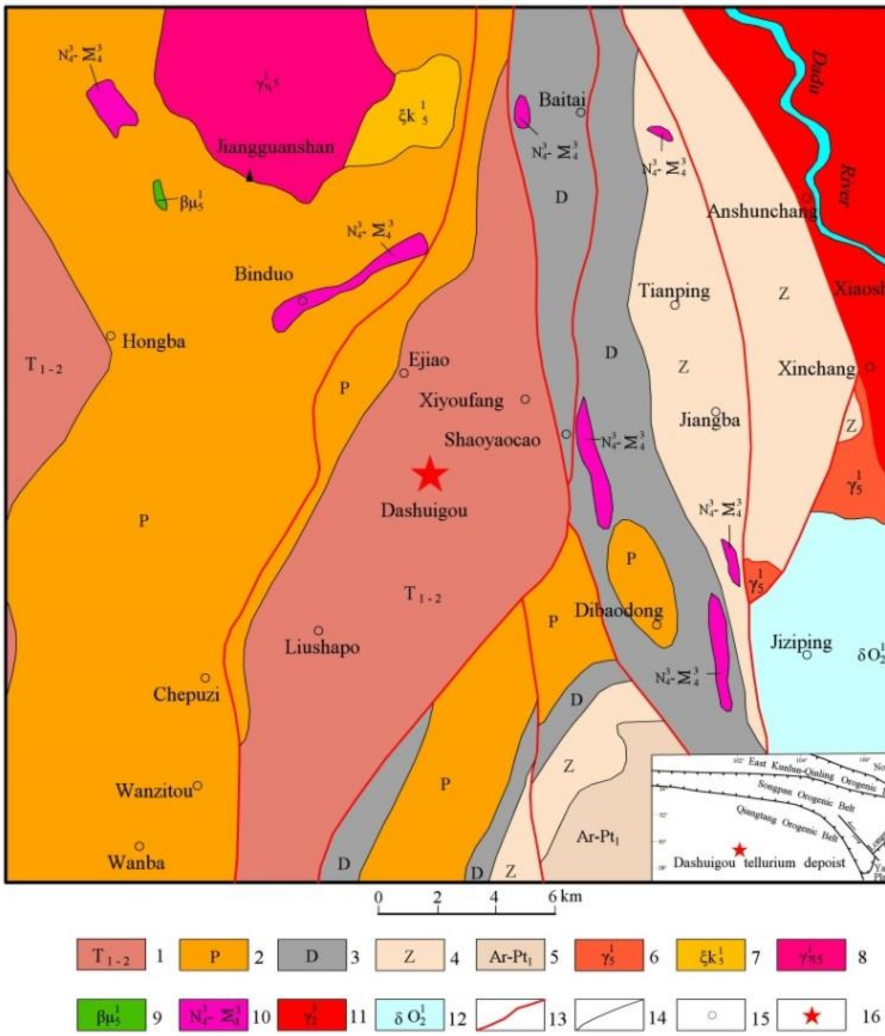

Figure 2. Regional geology[4 & 28-29]

1. The lower and middle Triassic metamorphic rocks; 2. The Permian metamorphic rocks; 3. The Devonian metamorphic rocks; 4. Metamorphic rocks of the Sinian system; 5. Metamorphic base complex of the Archean Kangding group; 6. Plutonic granite of the Indosinian orogeny; 7. Plutonic alkaline syenite of the Indosinian orogeny; 8. Plutonic monzonitic granite of the Indosinian orogeny; 9. Hypabyssal sillite of the Indosinian orogeny; 10. The late Hercynian basic-ultrabasic rocks; 11. The late Proterozoic plutonic granite; 12. The early Proterozoic-Archean plutonic quartz diorite; 13. The deep and large fault; 14. The geological boundary; 15. Village and/or town; 16. The tellurium deposit.

2.2 Strata

Deeply affected by the north-south uplift zone, the strata, igneous rocks and various geological structures in this area are distributed in nearly north-south strips (Fig. 2). The strata exposed in the study area are mainly a series of shallow metamorphic rocks from the Sinian, Devonian, Permian, and lower- middle Triassic systems (Fig. 2 and Table 1). A large area of Kangding group metamorphic rocks is exposed to the southeast of the study area, which is recognized as the oldest rocks in the Xikang-Yunnan or Kang-Dian geo-axis of the second level geotectonic unit of the Yangtze paraplatform, that is, the metamorphic crystalline basement[4,16-18 & 28-36].

Table 1. Summary of regional stratigraphic sequence, sedimentary formation, and lithology in the study area[4 & 28]

Geological time			Tectonic layer	Sedimentary formation and lithology	Note
Era	Code	System			
Cenozoic	Q	Quaternary	Himalayan tectonic layer	The upper part is the alluvial layer, the middle part is	
				the glacial layer, and the lower part is the mixed	
				sedimentary layer of alluvial, slope and glacial deposits.	Unconformity
Mesozoic	$T_{1\text{-}2}$	Lower-Middle Triassic	Cover	Marine carbonate and basic volcanic rock sedimentary	contact
				formations, which have been metamorphosed to marble	
				, slate and schist.	Conformity or
Paleozoic	P	Permian		The upper part is formed by clastic rocks, marine carbonate	fault contact
				and basic volcanic rocks, and the lower part is formed by	
				marine carbonate; it has been metamorphosed into slate,	Conformity or
				marble and schist respectively.	fault contact
	D	Devonian		The upper part is formed by marine carbonate, and the	
				lower part is formed by clastic rock and marine carbonate,	Fault or/and
				which has been metamorphosed to marble and slate, etc.	pseudoconformity
Proterozoic	Z	Sinian		Formation of marine carbonate and clastic rocks, which	contacts
				have been metamorphosed to marble and slate, etc.	
	Pt_1	Kangding Group metamorphic complex	Crystalline Basement	Basic, medium and acid volcanic rock formations and	Angular
Archean	Ar			flysch-like formations; have been subjected to regional	unconformity
				dynamic metamorphism, becoming high greenschist facies	and fault
				and amphibole facies metamorphic rocks.	contact

The crystalline basement, also known as the Kang-Dian complex or Kang-Dian gneiss, is now commonly known as the Kangding group and is a set of moderately to deeply metamorphosed and migmatized rocks. This set of rocks extends intermittently in a north-south direction in the western Panzhihua region, stretching for over 400 kilometers. They are clearly controlled between two lithospheric fault zones, forming a distinct north-south uplift zone.

The lower part of the Kangding group is composed of thick hornblende rocks, while the middle part is composed of biotite granulite, hornblende granulite, and biotite schist. The upper part is sandwiched with granulite and shallow granulite. The phase transition is obvious from north to south. The upper part of the Kangding group is mainly composed of mica schist and biotite granulite, interspersed with siliceous marble, dolomite marble, granulite and quartzite. The lower part of the Kangding group's protolith is mainly composed of tholeiitic basalt erupted from the sea floor, and gradually changes upward into calc-alkaline and medium-acidic volcanic rocks, and flysch and/or flysch-similar formations. The Kangding group has experienced regional dynamic thermal metamorphism of high greenschist facies and amphibolite facies, accompanied by acidic, basic and ultrabasic magma intrusions during the metamorphism. In addition, this set of rocks also suffered intense migmatization and granitization. The isotopic age of this set of rocks is 2,950~1,700 million years.

The late Proterozoic and early Sinian were the transitional period when the study area entered the stable platform development stage. Beginning in the late Sinian, the Kang-Dian geo-axis entered the stage of stable platform development and began to receive platform cover deposition. As the first true platform cover of the Yangtze paraplatform, the upper Sinian is widely distributed in the region and has stable thickness. It generally overlies the folded metamorphic basement in an angular unconformity (Fig. 2 and Table 1). During the early Paleozoic, the

Earth's crust frequently experienced vertical ups and downs, resulting in the absence of the Cambrian, Ordovician and Silurian systems in this area. During the Devonian and Permian periods, the entire region experienced widespread subsidence and seawater intrusion, depositing a carbonate-clastic rock series.

The upwelling of upper mantle magma causes thermal doming of the crust. Accompanying this process, basic-ultrabasic magma from the upper mantle intrudes into the crust along resurrected faults. During the Carboniferous, this area was uplifted, resulting in the loss of this set of strata.

From the late Permian to the middle Triassic, the upper mantle magma upwelling in the area reached a climax. Accompanied by faulting activity, Hercynian Emeishan basalts (260-254 Ma) and layered iron-rich basic-ultrabasic rocks containing vanadium-titanium magnetite from the upper mantle, as well as Indosinian granites (257-205 Ma) , intruding or erupting along the ancient faults resurrected in the crystalline basement, forming a set of north-south tectonic-magmatic mixed complex belts developed on the crystalline basement in the area. Most of the cover rocks of different ages in the area have experienced regional low-temperature dynamic metamorphism and became phyllite, schist, and marble.

2.3 Igneous rock

The igneous rocks in the area are relatively developed, widely distributed and of various types, including ultrabasic, basic, neutral, alkaline, and acidic igneous rocks. These igneous rocks were active to varying degrees during the Zhongtiao (Ar-P_{t1}), Chengjiang (Z_1), Caledonian (Z_2-S), Hercynian (D-P), Indosinian (T_{1-2}), Yanshanian (J_{1-2}-K_2) and Himayalan (R-Q) orogeny or period. Among them, the Zhongtiao period - Chengjiang period and the late Hercynian (P) - Indosinian periods are the two peak periods of igneous activity in this area, which are briefly described as follows[4,10,16,28 & 30-31]:

The magmatic activity during the Zhongtiao orogeny was intense. In the early stage, there was a large-scale submarine volcanic eruption, accompanied by the intrusion of basic-ultrabasic magma. In the middle stage, sodium granite was intruded. And in the later stage, a little potash granite was formed. Among them, the representative intrusion is the Archean - early Proterozoic Jiziping-Caluo granite extending north-south, covering an area of 55 km^2. These igneous rocks were later metamorphosed together to form the crystalline basement of the Kang-Dian complex (Fig. 2).

In the area, granite and alkaline intrusive rocks developed during the Chengjiang orogeny. The typical representative is the late Proterozoic Xiaoshui granite exposed in the eastern portion of the study area and distributed in a north-south direction across a huge area of 950 km^2 (Fig. 2). As a typical orogenic product, the batholith produced iron, tin, and tungsten ore bodies in some of its parts; and Ta, Nb, and Y showings in the alkaline granites.

Magmatic activity in this area formed a new climax during the late Hercynian (P) and Indosinian (T_{1-2}) periods. In the late Hercynian orogeny, a large amount of basalt was ejected along the north-south fault zone, which is the famous Emeishan basalt. At the same time, a large number of mafic-ultramafic intrusions, diorite and granite were intruded along the north-south deep faults. The basic-ultrabasic intrusive rocks exposed in the form of rock bed, sheet, and dyke in the eastern and northwestern parts of the study area. Tremolite and asbestos are often enriched in certain kinds of intrusive rocks, magnetite is enriched in other intrusive rocks, and some intrusive rocks have copper and nickel mineralization. Among them, the Binduo and the Shaoyaocao stocks are two relatively large rock stocks. Geological and geochemical data show that these basic-ultrabasic intrusive rocks originated in the upper mantle, which are directly related to the Xiaojinhe lithospheric fault zone.

All intrusive bodies developed in the area during Yanshanian orogeny (J_{1-2}-K_2) are granite, and representative rock bodies include Jiangguanshan alkaline syenite, Jiangguanshan quartz diorite, and Xinchang granite (Fig. 2).

There are a large number of quartz veins, carbonate veins, and diabase veins in the study area’s various metamorphic rocks and intrusive rocks of different ages, as well as a small amount of granitoid aplite, granite pegmatite, and lamprophyre dikes, etc.

2.4 Structure

Faults and fault zones are well developed in the study area, most of which are deep and large faults that cut through the lithosphere in a north-south or nearly north-south direction and reach the upper mantle or asthenosphere. They are channels for upwelling material including ore-forming minerals from the upper mantle. These deep and large faults are often composed of mylonite zones and have the characteristics of ductile shear zones[4,10,16 & 28]. The representative fault zones are briefly described as follows:

Xiaojinhe or Jinping-Muli fault zone: The fault zone spans Yunnan and Sichuan provinces, along the Xiaojinhe River and Jinping Mountain to Xiyoufang of Shimian County in the study area. It is more than 250 kilometers long and is the dividing line between the Songpan-Ganzi geosyncline and the Yangtze paraplatform. There are compression tectonic zones developed near the fault zone, and many recorded earthquakes have occurred in the Muli area.

As part of the Yulong-Longmen fault zone, the Xiaojinhe fault zone was the dividing line between the eastern paraplatform and the western geosynclinal area during the Paleozoic-Triassic period, and has been the southeastern boundary of the Qinghai-Tibetan Plateau since the Cenozoic. According to plate tectonic theory, this fault zone is a plate suture line.

Anninghe fault zone: This fault zone is located on the western edge of the Yangtze paraplatform, starting from Jintang in the north and extending south along the Dadu River to Shimian County. It passes through Mianning, Dechang, and Huili, crosses the Jinsha River and enters Yunnan to connect with the Yimen fault, running through the Kang-Dian geo-axis.

The fault zone has been active multiple times, with basic to ultrabasic rocks distributed along the fault zone, and abundant mineral resources on both sides of the fault zone.

Similar fault zones include the Mopanshan, Jinhe-Chenghai, and Xiaojiang deep and large fault zones.

In addition to the linear structures mentioned above, there are also numerous circular structures in the area. Remote sensing interpretation shows that both linear and annular structures develop in the study area. The annular structure is strongly intersected by linear structures with different directions and different mechanical properties, forming the Ø-shaped structures that are very favorable for mineralization (Fig. 3) [4,16, 25-26, 28 & 36].

2.5 Regional minerals

The favorable geotectonic setting and well-developed tectonic and magmatic geological conditions have created abundant mineral resources in the study area. These mineral resources are both endogenous and exogenous. The economic value of Fe, Ti, V, Cu, Pb, Zn, rare element, rare earth, asbestos, and coal is the most prominent; among which internationally renowned mines include Panzhihua vanadium titanium magnetite and asbestos mines[4 & 28].

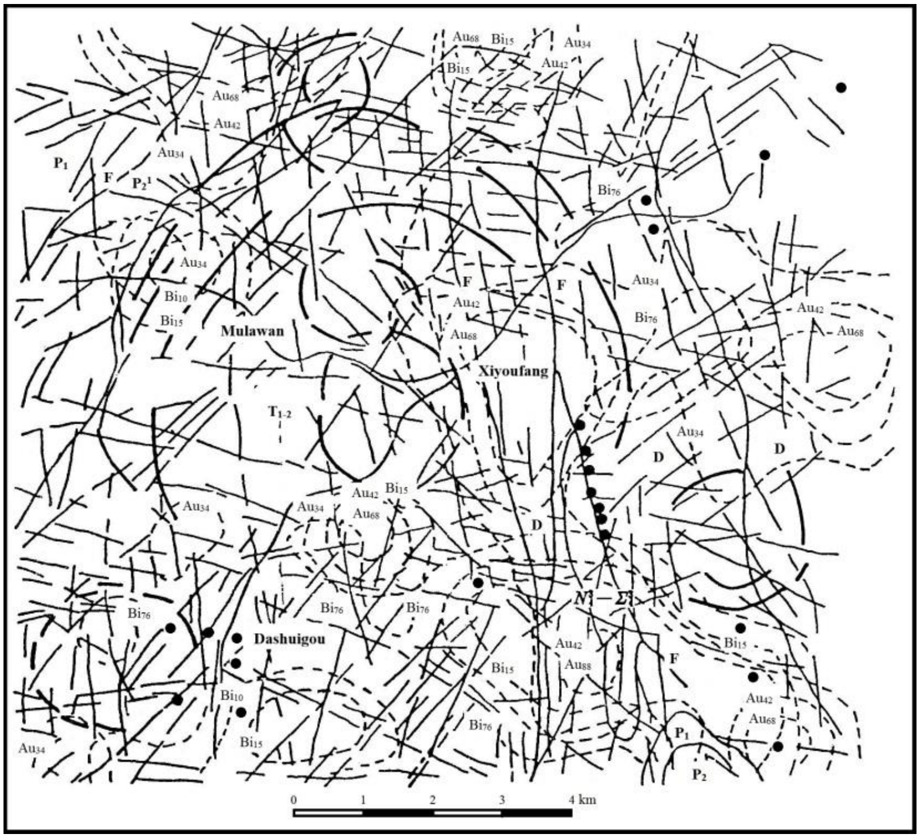

Figure 3. Linear-circular structures based on remote sensing satellite image and geochemical anomalies in the study area[2 & 37]

The endogenetic deposits within the area include:

- Cu, Ni, and Pt deposits related to ultrabasic rocks;
- Fe, Ti, V, P, Cu, Ni, Cr, and Pt deposits related to layered mafic-ultramafic complexes;
- Fe and Cu minerals related to basalt;
- Nb, Ta, Zr, Hf, U, and Th deposits related to the group of alkaline dykes;
- Nb, Ta, Y, Zr, and Hf minerals related to alkaline granite;
- La, Ce, Th, U, Mo, Cu, Pb, Zn, fluorite, and gold deposits related to potassium feldspar granite;
- Hydrothermal iron ore associated with gold;
- Hydrothermal copper, lead, zinc, and gold deposits;
- Hydrothermal quartz vein type lead, zinc, and gold deposits;
- Chrysotile asbestos deposits related to late Proterozoic ophiolite;
- amphibole asbestos deposits related to Permian ultrabasic rocks

The exogenous mineral deposits within the area include:

- Hematite deposits associated with the Triassic sedimentary rocks that has been modified by regional metamorphism;

- Quaternary placer gold deposit;
- Perlite mineral deposits produced in the Devonian system;
- Slates produced in the Triassic system, gypsum, and coal that are widely used by local people.

3 Deposit geology

3.1 General background

The Dashuigou independent tellurium deposit is located near the west side of the above-mentioned Xiaojinhe deep fault zone and at the northern edge of the Panzhihua-Xichang rift (Figs. 2 and 3). The structure of this area is north-northeast-oriented, with common tight folds and inverted folds. Therefore, the strata and igneous rocks in this area are also distributed in a north-south or nearly north-south direction[4,16 & 28].

Geotectonically, the mining area is located in the Jiulong geoanticline, a third-level tectonic unit extending north-south in the Songpan-Ganzi geosynclinal fold belt. The Jiulong geoanticline and all other adjacent geotectonic units are bounded by various deep faults. For example, the eastern part of the Jiulong geoanticline is connected to the Kang-Dian geo-axis by the Xiaojinhe fault.

According to the results of seismic sounding and regional gravity data, the mining area is located in the transition zone between the western mantle depression area and the eastern mantle platform area; that is, the Wenchuan-Shimian-Muli mantle slope zone. It is essentially a west-dipping steep slope of the Moho surface. It is also the transition zone and dividing line between the Songpan-Ganzi fold belt and the Yangtze paraplatform.

3.2 Strata

Devonian and Permian strata expose near the periphery of the mining area[4,16,28,30-33 & 36-38].

The Devonian strata are mainly marine carbonate rocks that have suffered medium-pressure regional dynamic metamorphism, most of which is marble.

The contact fracture zone between the Devonian and Sinian systems contains Cu, Au, and Ag minerals of a certain scale, such as the Dayanfang Cu-Au-Ag mine, the Jinjitaizi Cu-Au mine, and the Guangjinping gold mine etc.

The Permian system is well developed near the mining area, with a wide exposure area and a long and narrow strip extending from north to south. The lower series of the Permian system is a set of fossil-rich carbonate rocks, while the upper series includes thicker basalt, clastic rocks, argillaceous rocks, and carbonate rocks. This set of rocks suffered medium-pressure regional dynamic metamorphism during the Indosinian orogeny and became greenschist phase metamorphic rocks.

The Triassic strata in the study area is a set of littoral-neritic phase carbonate-basic volcanic rocks, but has suffered regional low-temperature dynamic metamorphism in the Indosinian orogeny and turned into low greenschist phase metamorphic rocks, including marble, phyllite, and schist (Fig. 4).

The Triassic system in the study area is exposed in two parts, one is to the west of Hongba on the west side of the mine, and the other is the diamond-shaped block of the Dashuigou mine itself. Some geologists call it the Xiyoufang-Liushapo tectonic block. The direct host rock of the tellurium ore bodies in the deposit is the Triassic phyllite, schist and slate, in which exists a well-developed 10-15 m wide fault zone, in which an approximately 3 m wide tourmaline-quartz vein develops. Strong pyrrhotite alteration occurs along both the hanging wall and footwall of the fault zone (Figs. 4 and 5).

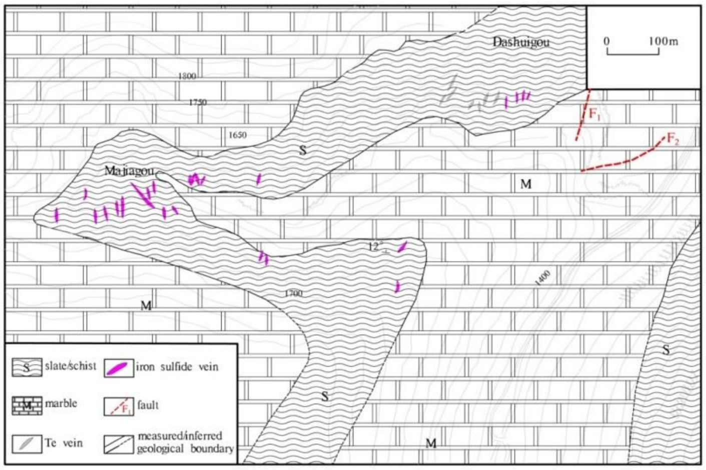

Figure 4. Deposit geology[4 & 28]

The Triassic stratigraphic sequence of the Dashuigou tellurium deposit is as follows (Figs. 4 and 5)[4,28 & 38-41]:

i. Schist, phyllite and slate formation at the top
ii. large-thick fine-grained marble in the upper part
iii. schist, phyllite and slate formation in the middle
iv. fine-medium grained banded marble in the lower part
v. coarse grained thick marble at the bottom

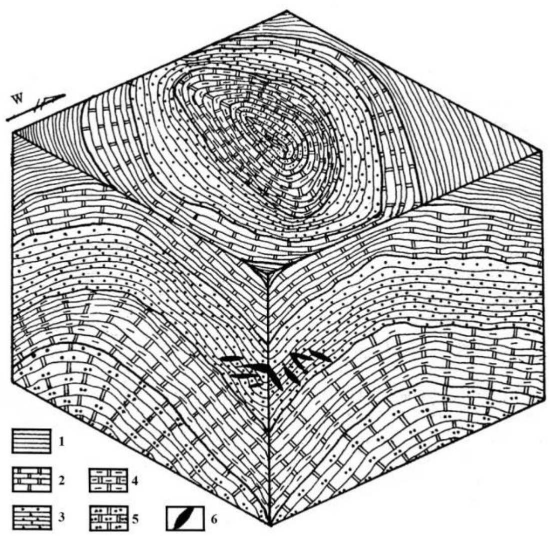

Figure 5. Schematic diagram of the ore bodies' 3D distribution of Dashuigou tellurium deposit

1. The upper phyllite, schist and slate of the lower-middle Triassic system; 2. The thick marble in the upper part of the lower-middle Triassic system; 3. The middle phyllite, schist and slate of the lower-middle Triassic system; 4. The banded marble of the lower-middle Triassic system; 5. The lower coarse-grained marble of the lower-middle Triassic system; 6. The tellurium ore body

The phyllite, schist and slate overlying the banded marble are pushed and compressed along the contact between the two, forming an interlayer compression fold (Fig. 6). This contact is also basically the bottom boundary of the tellurium vein.

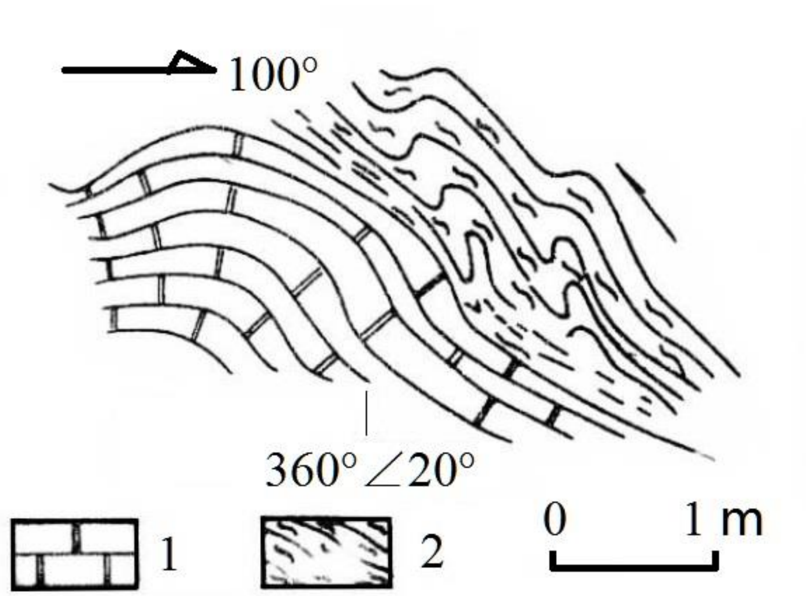

Figure 6. Sketch of reverse compression fold between banded marble and phyllite/schist/slate

1. The banded marble; 2. The phyllite/schist/slate host rocks of the tellurium ore body

The main host rocks of the ore bodies include hornblende schist, garnet schist, tourmaline schist, and chlorite schist (Fig. 7). Other minerals in the schist/phyllite/slate include quartz, plagioclase, potassium feldspar, muscovite, rutile, and magnetite. According to its geological, mineralogical, petrographic, petrochemical, and geochemical characteristics, the protolith of this set of rocks is mainly poorly differentiated mantle-derived basic volcanic rock.

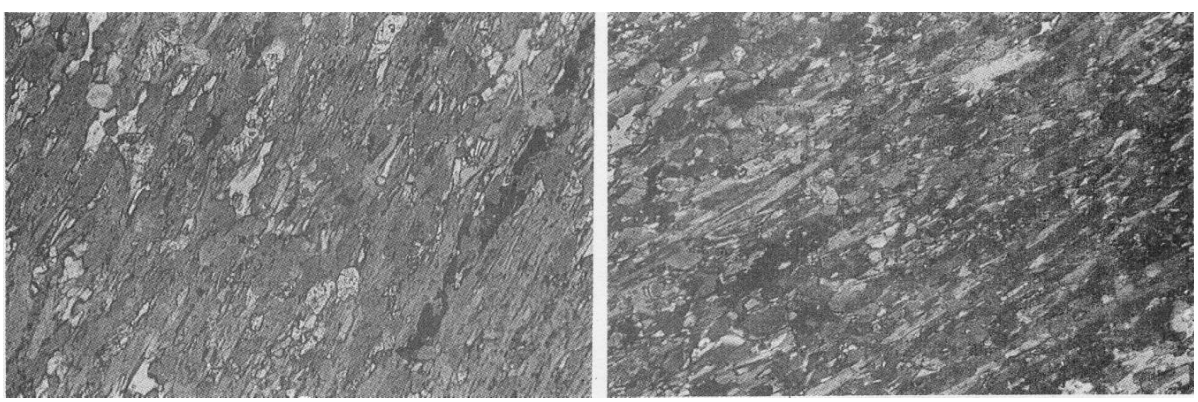

Figure 7. The middle ore-hosting hornblende schist (left) and chlorite schist (right) of the lower-middle Triassic system

(The thin section (−) 3.3 × 10)

This set of rocks has a low SiO_2 content ranging from 32.3% to 52.12%, with an average of 43.71%. Al_2O_3 ranges from 12.54% to 16.75%, with an average of 14.15%. Low Na_2O (<4.00%) and K_2O (average content generally comparable to Na_2O). Its total iron $FeO^*/(FeO^* + MgO) = 0.68$, $CaO/Al_2O_3 = 0.70 < 0.82$, $Fe^{3+}/(Fe^{2+} + Fe^{3+}) = 0.23 < 0.40$, indicating the nature of mantle derived basic volcanic rocks[4 & 28].

3.3 Structure

The Triassic strata make up a NNE-trending dome, namely, the Dashuigou dome. The deposit is located at the northeastern end of the Triassic metamorphic dome. The ore bodies are both controlled by and fill a group of shear fractures (Figs. 4 and 5)[4 & 28].

Both faults and folds are well-developed in the area. The annular and linear structures together make up special Ø-shaped structures which control the formation of different types of endogenetic mineral deposits, including the Dashuigou tellurium deposit (Figs. 3, 4 and 5).

Linear structures can be divided into the following groups: NW, NNE, NS, NWW, and NEE. These linear structures include the Dadu River ductile shear zone and the Xiyoufang ductile shear zone (Figs. 2, 3 and 4).

As the area’s largest known annular structure concentric with the Xiyoufang as the center at a diameter of about 8 km, the Xiyoufang annular structure (Fig. 3) is closely related to mineralization. More than 20 tellurium showings and the Dashuigou tellurium deposit, as well as more than 10 Au-Bi composite geochemical anomalies and some gold geochemical anomalies, are spatially related to the annular structure. With its southern point reaching the Dashuigou deposit, the Xiyoufang annular structure is a composite ring. In addition to the concentric composite ring of the large ring itself, there are two small annular structures with a diameter of about 2 km inside the large ring. It is also accompanied by two other small rings around it.

Located in the southwest of the Xiyoufang annular structure, the Dashuigou annular structure is one of the sub-rings of the Xiyoufang annular structure and intersects with NE, EW, SN, and NW trending linear structures, forming a characteristic Ø-shaped structure and controlling the Dashuigou tellurium deposit and the nearby Majiagou tellurium showing, as well as several Au and Bi geochemical anomalies. The perfectly circular Jinhuadong annular structure is also a sub-ring of the Xiyoufang annular structure and intersects with NWW, NNW, and SN-trending linear structures, forming a characteristic Ø-shaped structure, and controls the Jinhuadong, Qifenyao, and Bafenyao tellurium showings, as well as several Au and Bi geochemical anomalies. In addition, there are Baita, Tianwan Township, Tangjiapo, and Jiangguanshan ring structures. The common feature of these annular structures is their close spatial relationship with the Bi and Au geochemical anomalies.

There are two large ductile shear zones in the area that form the basic structural framework, which are briefly described as follows.

The Dadu River ductile shear zone, which extends along the west bank of the Dadu River, is over 300 kilometers long and has a maximum width of over 30 kilometers. It is distributed in a north-south direction and is located in the northeast of the Dashuigou tellurium deposit. The fault zone converges in the north and spreads in the south, affecting a range of approximately 10-15 kilometers from east to west in the areas of Xiyoufang, Dashuigou, and Jinhuadong (Figs. 2 and 3). This fault zone controls most of the metal deposits discovered in the research area.

The Xiyoufang ductile-brittle shear zone has a total length of over 300 kilometers and a width of 10-15 kilometers. The Dashuigou sub-zone is the main structural zone of the Xiyoufang ductile-brittle shear zone. This sub-zone is composed of several roughly parallel secondary zones, with the largest one passing through the Dashuigou and Majiagou tellurium deposit and/or showing, while the remaining secondary zones pass through the other tellurium showings.

The above two ductile shear zones intersect in the northeast of the mining area and are also part of the Xiaojinhe lithospheric fault zone mentioned above.

Other representative faults in the study area include the Hongba fault, Wanbahe fault, Xiyoufang-Guanyinshan fault, Keluo-Jiziping fault, and Anshunchang-Xinchang fault from west to east, which are part of the two shear zones mentioned above. On the whole, these faults are broom-shaped converge at the northern end, and spread out at the southern end.

The folds in the study area are mostly NNE or nearly SN-trending, and are relatively tight, narrow, and long. These folds include the Dashuigou dome structure and the Bindo anticline in the northwest of the deposit, etc.

The Dashuigou dome is roughly NNE trending, more than 10 km long, and entirely composed of lower and middle Triassic metamorphic rocks. Its northern section is damaged by a fault of nearly the same strike, and its four sides of the northeast, southwest, northwest, and NNW are cut and bounded by NNW-trending, near north-south, and NNE-trending faults respectively, forming a highly flattened rhombic block in space. On the two-dimensional plane, the Dashuigou tellurium deposit is located in the north-central part of the dome.

3.4 Igneous rock

No large intrusive rocks occur within a 5 km radius around the deposit. Only two small Permian ultrabasic-basic rock bodies emerge within a 10 km range of the deposit as described above (Figs. 2 and 4).

4 Ore body

The Dashuigou tellurium deposit is produced at the north-eastern end of the dome consisting of the lower-middle Triassic system (Figs. 2-5). The entire tellurium ore bodies are limited to the tourmaline-containing amphibolite schist in the middle of the dome (Figs. 4 and 5).

Both the early pyrrhotite and late tellurium ore veins filled in a group of structural fissures with shear properties and intersected obliquely with the ore-hosting rocks. The early-formed pyrrhotite veins are in a typical lens shape, in which the breccia of the ore-hosting rock is common (Figs. 8 and 9) [4, 28 & 40-42].

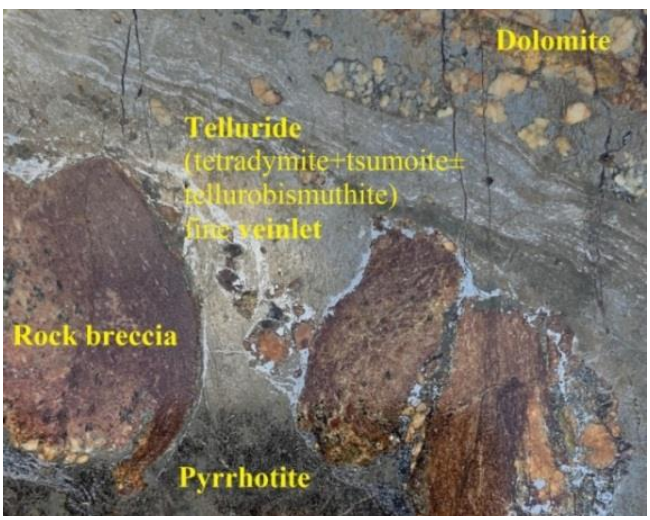

Figure 8. The lead grey-silvery telluride (tetradymite + tsumoite ± tellurobismuthite) fine veinlets + dolomite (brownish white) + host rock breccia (brown) in massive pyrrhotite (grey) from the deposit

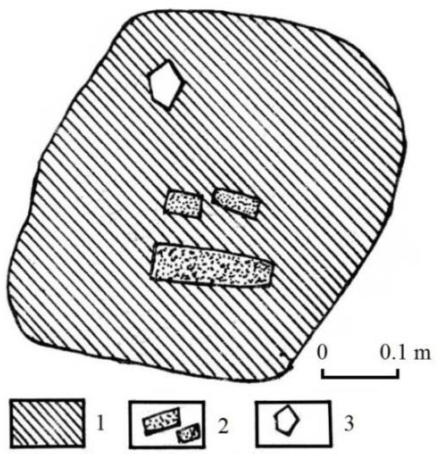

Figure 9. Sketch of country rock breccia and megacrystalline pentagonal dodecahedron pyrite in early pyrrhotite veins

After the formation of early pyrrhotite veins, they were subjected to compressive shear activities and fractured to form expansion structures. Late tellurium veins and/or veinlets filled these fractures (Figs. 8 and 10).

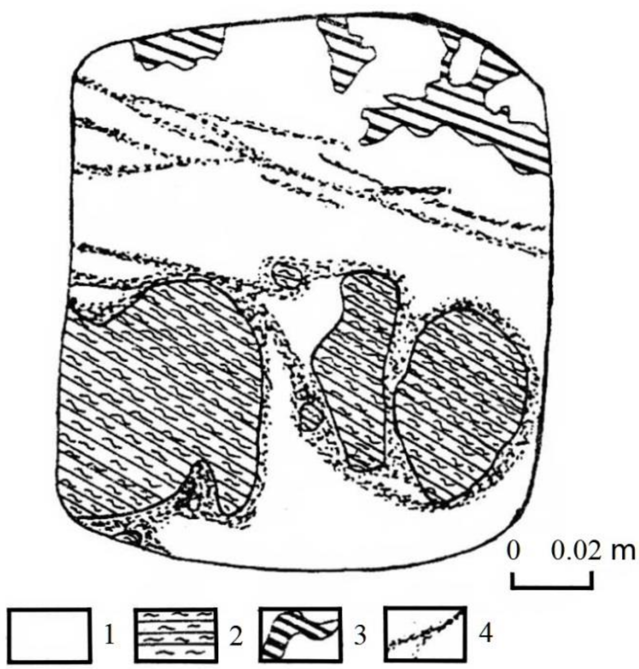

Figure 10. Sketch of the late telluride veinlets surrounding country rock breccia in early pyrrhotite vein

Table 2 briefly lists the basic characteristics of representative tellurium ore bodies in the Dashuigou tellurium deposit.

Table 2. Basic characteristics of representative tellurium ore bodies in Dashuigou tellurium deposit

Ore body	Occurrence	Length	Width	Thickness	Grade	Note
		Unit: meter				
I-1	280°∠60°, lateral direction 342°, lateral angle 15°	61.0	8.0	0.3	0-34.5%, average 6.0-7.0%	The lateral direction of the ore body refers to the orientation of the ore body axis, and the lateral accretion angle is the angle between the ore body axis and the horizontal plane.
I-2	300°∠70°, lateral direction 5°, lateral angle 22°	30.0	7.0	0.3		
I-3	300°∠60°, lateral direction 15°, lateral angle 12°	10.0	2.5	0.1	Average 0.0-0.5%	
I-4	335°∠60°, lateral direction 27°, lateral angle 33°	16.0	5.0	0.4		
I-5	285°∠55°, lateral direction 333°, lateral angle 15°	26.0	6.0	0.3	Upper part: 90.0%, lower part: 0-0.5%	
I-7	288°∠49°, lateral direction 340°, lateral angle 15°	-	-	0.2	-	
I-8	280°∠51°, lateral direction 330°, lateral angle 20°	-	-	0.5	-	
I-9	268°∠83°, lateral direction 330°, lateral angle 20°	-	-	0.3	-	
I-10	295°∠68°, lateral direction 355°, lateral angle 24°	-	-	0.6	-	

The overall occurrence of the tellurium ore zone composed of all tellurium ore bodies is 280°∠55°-70°, with a general strike of 10°±, an axial direction of 240°, and a lateral angle of 20°±. The entire ore zone is 25-30 meters wide and its axial length about 40 meters (Table 2).

The single ore bodies generally trend 350°-10° and/or 20° and dip 45°-83° westward, while the occurrence of host rocks in the mining area is 8°-38°∠21°-35°. The two are obviously obliquely related (Figs. 4 and 5).

Among all ore bodies, #I-3 ore body is special. It is almost entirely composed of dolomite and various tellurides, and the tellurium minerals mostly appear in the form of coarse grained scales, and there are no other sulfides such as pyrrhotite and pyrite commonly found in other ore bodies. The dolomite in #I-3 ore body is milky white, and tellurium minerals are distributed in a patchy pattern within the dolomite.

Except for the #I-5 ore body, the hanging and foot walls of all the other ore bodies are all schist. The hanging wall of the #I-5 ore body is schist, and the foot wall is banded marble; that is, the ore body is almost filled in the contact of the two different lithologies (Fig. 6).

The ore body appears in an obvious lens shape in the longitudinal section, and appears in the shape of veins and/or lenses arranged in echelon arrangement in the horizontal projection and plan views of different levels (Figs. 4 and 5). The echelon-like arrangement of tellurium ore bodies is particularly obvious in the 1450 m level (Fig. 11).

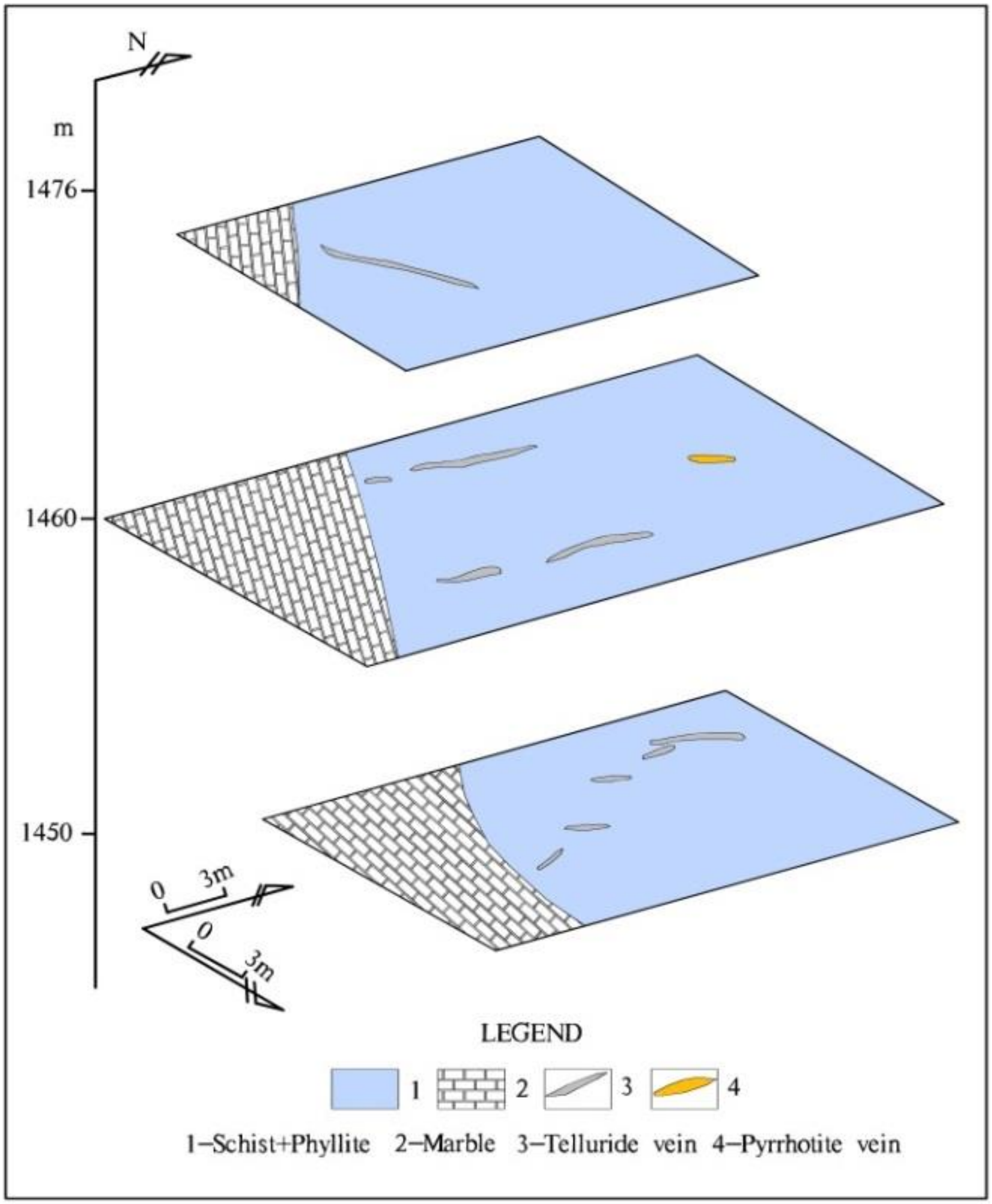

Figure 11. Three-dimensional spatial distribution of the tellurium ore bodies

Whether it is pyrrhotite veins or telluride veins, they all have a very striking and clear contact with the altered host rocks; that is, there is no gradual transition zone between these veins and the host rocks, and/or between the two different veins themselves (Figs. 12 and 17-19).

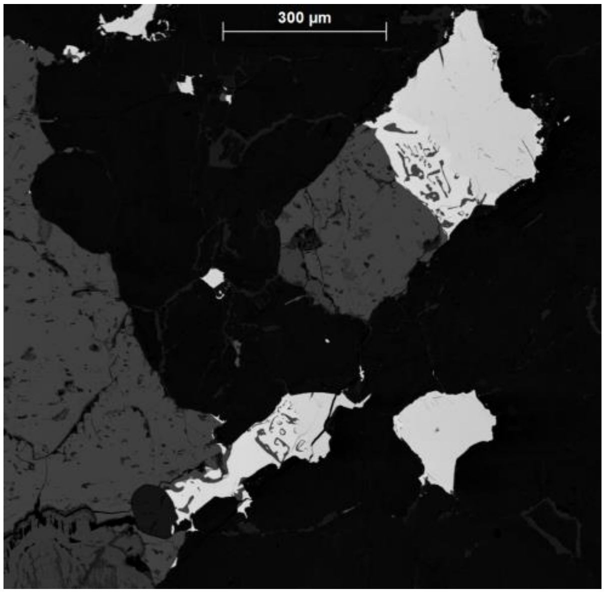

Figure 12. Distinct contact between pyrrhotite veins (dark grey), telluride veinlets (white), and carbonate veins (black)

5 Alteration and mineralization

Whether it is a pyrrhotite vein or a tellurium vein, the alteration zones on both sides are very narrow and non-zoned, which range between several centimeters and one meter in thickness. Those altered zones beside the massive and/or semi-massive ore veins are narrower, at only several centimeters wide. Field observations show that there is no positive correlation between ore body size and alteration intensity. This may be related to the fact that the mineralization of this deposit is narrow vein style[4 & 28].

The alteration zones are light gray or yellowish brown, obviously lighter than the surrounding host rocks of the same lithology, and the baked edge is very clear.

There are many types of alteration, including biotitization, dolomitization, silicification, tourmalinization, potassium feldsparization, albite, chloritization, grenaitization, muscovitizaion and/or sericitization, pyrrhotization, pyritization, and calciteization, etc.

Among them, dolomitization is the most widely distributed in the entire study area. Dolomite veins are an important carrier of tellurium. Where dolomitization is strong, the tellurium content increases significantly. In many cases, dolomite, quartz and muscovite occur symbiotically and/or associated with each other.

Alterations such as dolomite and quartz are products of multiple phases. The dolomite formed in the early stage is coarse grained, iron stained and brittle (Fig. 8), while the late dolomite has fine particles and no iron staining. The quartz veins formed in the early stages are brown or light brown due to iron staining, and dense shear cracks develop in them (Fig. 13). The late quartz is white, with muscovite developing in it.

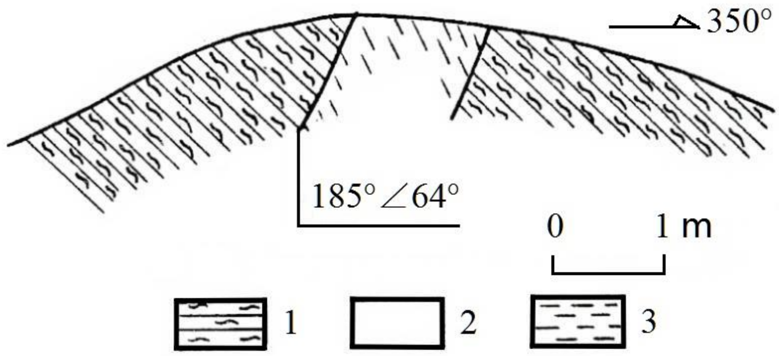

Figure 13. Sketch of dense shear fractures in the quartz veins in the mining area

1. Schist + phyllite, 2. Quartz vein, 3. Share fracture

The scaly biotite with intact crystal form forms fine veins or irregular clusters, closely attached to the early pyrrhotite veins, but has no spatial dependence with the late tellurium veins.

Ubiquitous in the study area, scale-like muscovite often appears together with the late quartz veins, or symbiotic with late dolomite in the form of veinlets. Occasionally, some muscovite appears superimposed on biotite on both sides of the early-formed pyrrhotite veins. This muscovite should be derived from the alteration of early biotite.

Tourmaline, chlorite and albite are closely symbiotic with the early-formed pyrrhotite veins. Mottled pyrrhotite and pyrite are often found in the flesh-red fine-medium grained albite veinlets.

Closely symbiotic with pyrrhotite, most, if not all of the pyrite appear in the form of pentagonal dodecahedrons with intact crystal forms (Fig. 14). The largest single crystal can reach several centimeters. It is certain that these pyrites are the product of the early paragenetic stage; namely, the pyritic stage. No pyrite is found in the late tellurium veins.

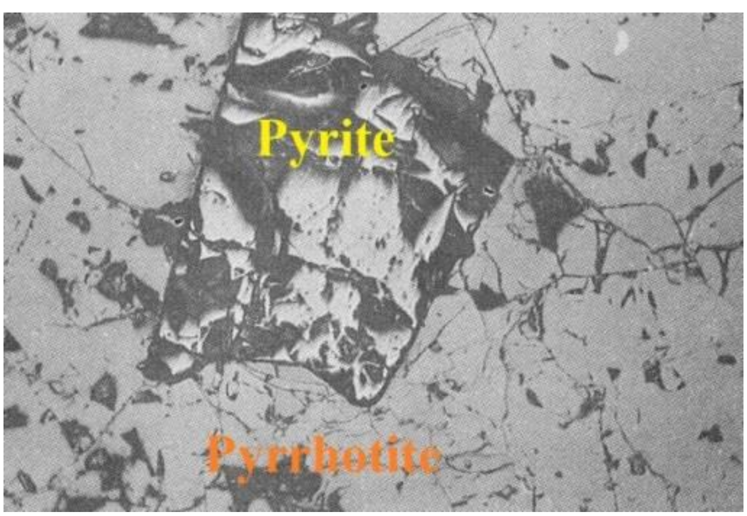

Figure 14. Euhedral pyrite (light grey) in massive pyrrhotite (grey)

(Thin section (−) × 200)

In contrast to pyrite, weaker chalcopyrite and galena mineralization should be products contemporaneous with the late tellurium mineralization. Under the microscope, tellurium minerals and chalcopyrite are commonly seen in association. Sometimes chalcopyrite veinlets can also be seen interspersed with telluride veinlets. Of course, it is also common to see chalcopyrite veins/veinlets interspersed with early-formed pyrrhotite veins.

Generally speaking, the alteration and mineralization in the mining area can be roughly divided into two groups: early and late, corresponding to the early and late mineralization stages respectively.

Early alteration and mineralization closely associated with pyritic (pyrrhotite + pyrite) veins include biotitization, dolomitization, silicification, tourmalinization, albite, chloritization, and pyritization. The typical symbiotic mineral combination is: coarse-grained iron-stained dolomite + megacrystalline pentagonal dodecahedron pyrite + pyrrhotite + biotite ± albite ± tourmaline ± native gold ± chalcopyrite.

Late alteration and mineralization closely associated with telluride veins include muscovitization, sericitization, dolomitization, silicification, calcite, chalcopyrite mineralization, gold mineralization, and galena mineralization, etc. Typical mineral combinations are tetradymite + tsumoite + quartz + dolomite + calcite + chalcopyrite + gold + silver.

6 Analytical method or methodology

This article uses the electron probe for line and surface scanning to qualitatively or quantitatively analyze ore samples, while also studying the existing forms of some elements and/or minerals.

The electron probe instrument can measure elements in the range of 4Be-92U, with a sensitivity of up to 3/100000 parts according to statistical views, and the actual relative sensitivity is close to 1/10000 to 5/10000 parts.

Generally, when the content of elements in the analysis area reaches 10-14 parts, it can be perceived. The measured diameter of the sample is within 1 μm and 500 μm.

Line scanning is the scanning of an electron beam along a straight line direction to determine the relative concentration changes of relevant elements in that straight line direction and obtain the concentration distribution curve. Surface scanning is the process of scanning a sample surface with an electron beam to directly observe and capture the type, distribution, and content of the element on the screen. This means that the concentration of the element is represented by the density of the white highlights in the photo (Fig. 17).

7 Geological dating

In order to further determine the temporal relationship between pyrrhotite veins and tellurium veins and determine the mineralization age of the Dashuigou tellurium deposit, the K-Ar isotope dating was conducted on different minerals in the deposit.

When collecting samples, in addition to paying full attention to their freshness, special consideration was also given to their reasonable spatial configuration.

One scaly biotite sample was collected from the hanging wall and another from the footwall of the telluride-free pyrrhotite vein. A superimposed altered muscovite sample was collected from the footwall of this pyrrhotite vein. In addition, a second muscovite sample was collected from the altered host rock beside one tellurium ore body. A third muscovite sample was collected from a dolomite vein at Miaoping on the periphery of the deposit. These pale greenish white scale-like muscovites appear in the form of veinlets in the large dolomite vein (Fig. 15).

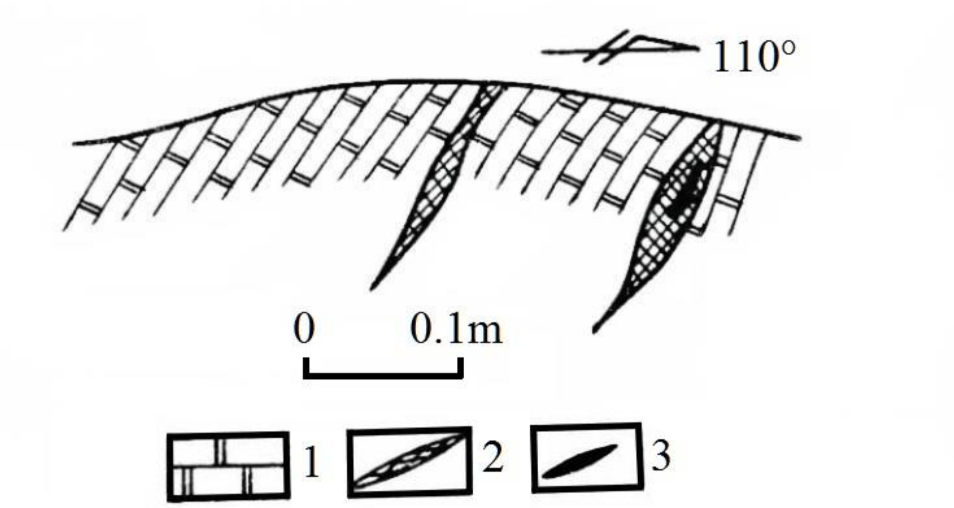

Figure 15. Sketch of the light greenish white muscovite veinlet in the coarse grained dolomite vein in the impure marble in the upper part of the ore-hosting bed at Miaoping near the deposit

1. Marble, 2. Dolomite vein, 3. Muscovite veinlet

The third muscovite sample was collected to verify whether the widespread muscovitization outside the mining area and the muscovitization in the deposit are the product of the same geological event. If it is the product of the same geological event, then muscovite, as an important alteration closely related to the tellurium mineralization, and one of the indicators of ore prospecting, can be given full attention when prospecting potential tellurium resource in areas with the similar geological setting.

A total of 5 mica mono-mineral samples mentioned above were carefully selected, separated, washed, dried, and then selected to ensure that their purity was above 99%. Finally, the K-Ar geological dating age was determined. The results are shown in Table 3 below.

Table 3. K-Ar isotope dating results of the Dashuigou tellurium deposit[4 & 43-44]

Series #	Sample ID	Sample description	Result (m.a.)
1	SD-19	Biotite in the hanging wall of the pyrrhotite vein without tellurium	177.7 ± 1.6
2	SD-20	Biotite in the footwall wall of pyrrhotite vein without tellurium	165.1 ± 1.5
3	SD-21	Muscovite in the footwall of the telluride-free pyrrhotite vein	88.3 ± 0.8
4	SD-23	Muscovite in the surrounding rocks near the No. 1 tellurium vein	80.2 ± 0.7
5	SL-09	Muscovite in dolomite veins outside the mining area	91.7 ± 0.8

It can be seen from Table 3 that, as speculated based on the geology above, the pyrrhotite vein and the tellurium vein are the results of two independent geological events with a long interval of geological time. The emplacement age of the former is 177.7-165.1 Ma, and its iconic wall rock alteration was biotitization. The latter is emplaced at 91.71-80.19 Ma, and its typical wall rock alteration is muscovitization/sericite.

8 Petrochemistry and geochemistry

Detailed petrochemical and geochemical studies of relevant rocks in the area show that protolith of the deposit's host rock is mantle-derived basic volcanic rock[4 & 28]. The contents of the main mineralizing elements Te, Bi, Se and Au etc. in different rocks of different geological times are very low, generally lower than or close to their respective crustal Clark values[1-4 & 28]. The enrichment of these elements is obviously related to alteration, the stronger the alteration, the higher the corresponding element content. Both the alteration and mineralization are most likely related to the upwelling of mantle materials produced through mantle plumes or mantle hot spots[4 & 28].

9 Ore

9.1 Mineral

According to the rock and ore identification under the microscope and electron probe analysis, there are more than 30 minerals that make up the ore. These minerals are mainly carbonates, silicates, sulfides including tellurides, native element minerals and a small amount of oxides. These minerals constitute different types of ores and waste rocks in different proportions, forms, occurrences, textures and structures[4,28,42 & 45-48].

Carbonate minerals are very developed and are produced in large quantities in both pyritic and tellurium stages. They are also one of the important carriers of tellurium minerals. The carbonate minerals in the deposit are mainly dolomite, calcite and siderite (Fig. 16).

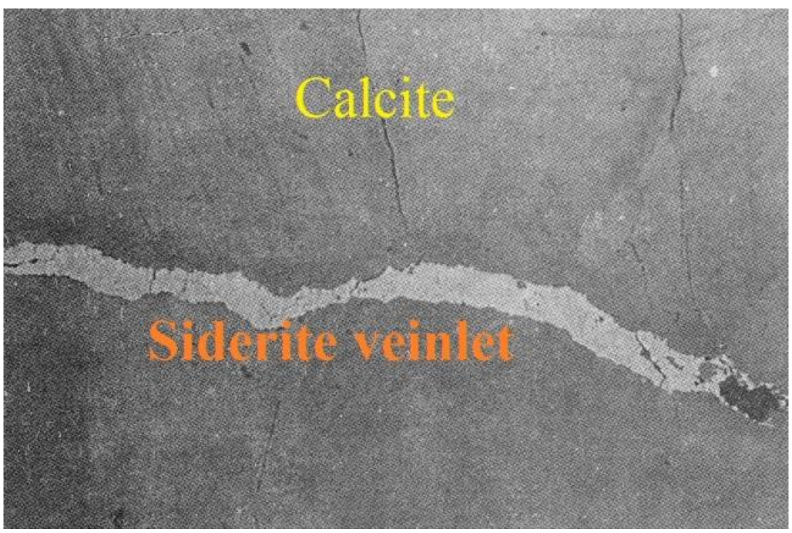

Figure 16. Siderite veinlet (white) interspersed with calcite vein (grey)

(Thin section (−) × 200)

Compared with the respective theoretical values of these three minerals[49], the dolomite in the deposit is poor in magnesium and rich in iron, but not to the extent of ankerite, so it can be called iron-bearing ankerite. Calcite is generally rich in magnesium and occasionally rich in iron, which can be called magnesium-bearing calcite and iron-bearing magnesium calcite respectively. The siderite is rich in calcium and slightly poor in iron. There exist isomorphic substitution series between $MgCO_3$ and $FeCO_3$. The composition characteristics of the above-mentioned carbonate minerals are also clearly reflected in various diagrams[4 & 42].

Silicate minerals are also the main gangue components in the deposit, which include muscovite, hornblende, plagioclase, chlorite, and potassium feldspar (Table 4). Among them, hornblende and plagioclase formed earlier, followed by chlorite and potassium feldspar, and muscovite including sericite formed later.

Oxide minerals include rutile, ilmenite, quartz, magnetite, specularite, hematite and limonite (Table 4). Except for quartz, which is mostly produced in the form of veins/veinlets, the other oxide minerals are mostly produced sporadically in the form of irregular granules and flakes.

Table 4. Electron probe analysis results of minerals from the Dashuigou tellurium deposit (wt. %)[4 & 42]

Sample #	Test point	SiO_2	Al_2O_3	CaO	K_2O	Na_2O	MgO	TiO_2	Cr_2O_3	MnO	FeO	Total	Mineral
II-2	1	0.22	0.10	0.39	0.00	0.00	0.00	98.05	0.05	0.08	1.00	99.89	tutile
	2	0.22	0.09	0.69	0.00	0.00	0.00	97.92	0.09	0.05	0.08	99.14	
	3	0.22	0.08	0.51	0.00	0.00	0.00	97.17	0.09	0.05	1.28	99.40	
	4	44.52	38.10	0.79	10.19	1.21	0.51	0.18	0.31	0.00	0.55	96.36	muscovite
	5	43.42	39.16	0.00	9.86	1.05	0.58	0.12	0.27	0.00	0.36	94.82	
I-4	6	43.91	14.62	13.45	0.00	1.02	9.81	0.01	0.00	0.12	14.87	97.81	amphibole
I-8	7	62.45	23.79	6.14	0.00	6.75	0.00	0.00	0.09	0.00	0.49	99.71	plagioclase
	8	0.13	0.00	0.02	0.00	0.00	1.80	53.32	0.04	0.93	43.34	99.58	Ilmenite
	9	0.13	0.00	0.12	0.00	0.00	1.80	52.20	0.04	0.93	43.21	98.43	
	10	38.61	15.94	13.01	0.13	1.38	8.85	0.37	0.04	0.16	13.67	92.16	amphibole
	11	27.17	21.94	0.09	0.00	0.00	19.18	0.10	0.19	0.11	15.36	84.14	chlorite
D4	12	46.93	38.28	0.04	6.67	0.91	0.22	0.26	0.08	0.00	0.57	93.96	
3	13	49.26	36.93	0.02	6.53	0.00	0.16	0.70	0.16	0.00	0.00	93.76	K-feldspar
	14	99.32	0.04	0.06	0.00	0.00	0.18	0.00	0.10	0.05	0.00	99.75	quartz
D1	15	0.25	0.00	1.77	0.02	0.31	0.31	0.00	0.02	0.01	90.57	93.26	magnetite
Sample #	**Test point**	**Te**	**Bi**	**S**	**Fe**	**Cu**	**As**	**Ni**	**Zn**	**Au**	**Ag**	**Total**	**Mineral**
D2	1	0.02	0.12	35.00	29.66	34.72	0.00	0.02	0.02	0.05	0.09	99.70	chalcopyrite
	2	0.00	0.21	37.57	61.33	0.07	0.02	0.10	0.02	0.00	0.00	99.32	pyrrhotite
	3	0.14	0.17	38.24	60.73	0.01	0.00	0.10	0.03	0.05	0.04	99.51	

Sulfide minerals are mainly pyrrhotite and pyrite formed in the early stage, with a small amount of chalcopyrite and galena formed in the late stage. Chalcopyrite is mostly interspersed in pyrrhotite in the form of veinlets, and galena blebs can be seen under the microscope.

Telluride minerals mainly include tetradymite (Bi_2Te_2S), tsumoite (BiTe), and tellurobismuthite (Bi_2Te_3)[4,7,42 & 48]. Among them, tetradymite accounts for over 90% of all the tellurides in the ore, while the latter two are mostly found in the contact metasomatic zone between tetradymite and pyrrhotite (Figs. 8, 10, 12 and 17-20).

Native element minerals mainly include native gold, electrum, kustelite, native silver, and native tellurium etc., as a series of minerals formed between gold and silver, as well as gold and tellurium.

According to other researchers[45-48], there are also small amounts of joseite, hessite, goldschmidtite, sphalerite, calaverite, stützite, vulcanite, secondary tellurium, and bismite etc. in the ore of the deposit.

To sum up, the minerals that make up the ore in Dashuigou tellurium deposit are as follows: tetradymite, pyrrhotite, pyrite, dolomite, quartz, chalcopyrite, tsumoite, tellurobismuthite, galena, magnetite, gold, silver, electrum, ilmenite, calcite, calaverite, siderite, mannesite, rutile, muscovite, biotite, sericite, hornblende, chlorite, plagioclase, K-feldspar, tourmaline, hematite, garnet, apatite, and epidote. The first five minerals comprise approximately 85% of the ore[4,7,40-42 & 45-48].

9.2 Structure and texture

The texture and structure of the ore are relatively simple and are briefly described as follows:

Texture

Euhedral - semi-euhedral flake: Mainly coarse-grained tetradymite appears in the form of relatively intact scales.

Euhedral: For example, coarse-grained pyrite appears as a typical pentagonal dodecahedron in pyrrhotite, dolomite and calcite veins (Fig. 14). Many times, coarse-grained dolomite and calcite also appear as euhedral crystals.

Xenomorphic-granular: Pyrrhotite and most quartz mostly appear in xenomorphic-granular in the deposit.

Metasomatic: Minerals formed early are metasomatized by late minerals and appear in the form of residues etc. (Figs. 8, 12 and 17-19).

Metasomatic graphic shows that telluride minerals such as tetradymite replace pyrrhotite and the latter's residue appears in the graphic form (Figs. 12 and 17-19).

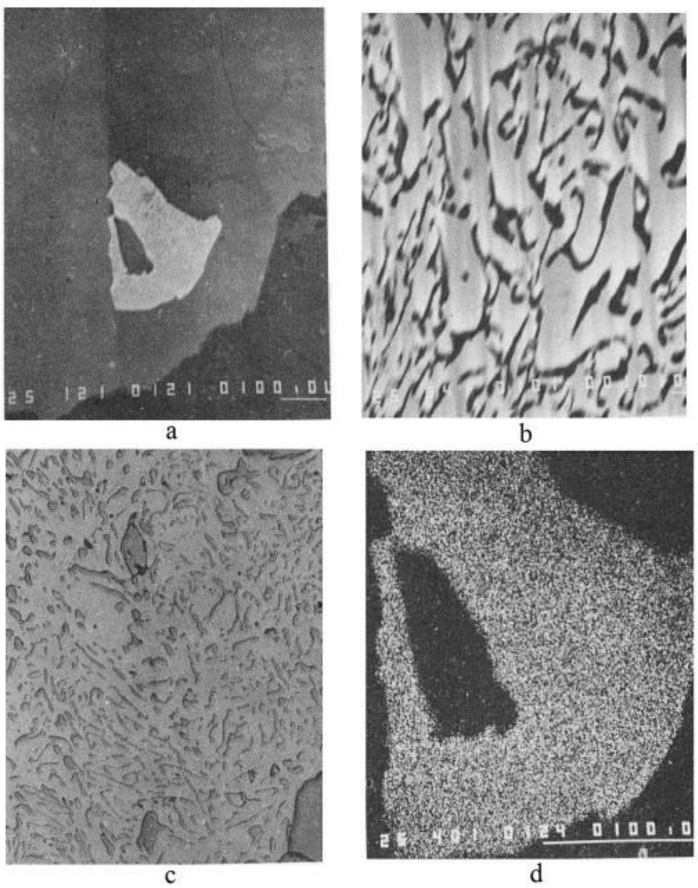

Figure 17. a~c: Reflection color and their mutual relationships between tsumoite (bright white), tetradymite (white), and pyrrhotite (grey to dark grey) in the back scattered electron image from the deposit (thin section (-): a ×120, b ×540, & c ×200). d: Te Kα X ray image indicating chemical composition distributions of telluride including tetradymite and tsumoite (white): the denser the white spots, the higher the Te content; the black colored background is pyrrhotite from the deposit (×400)

Reaction rim: Tetradymite reacts with pyrrhotite to form a unique reaction rim texture of tsumoite, and at the same time the above-mentioned metasomatic graphic texture appears (Figs. 12, 17a, 17d and 18-19).

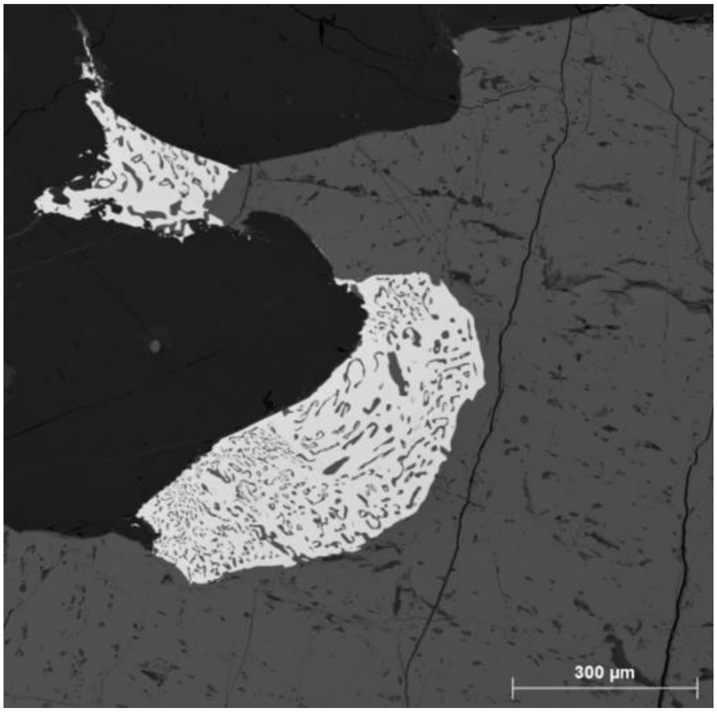

Figure 18. Reaction rim between telluride (tetradymite + tsumoite, white), pyrrhotite (grey), and dolomite (black)

Solid solution separation texture of tetradymite and chalcopyrite can be seen under the microscope (Figs. 12 and 17- 19).

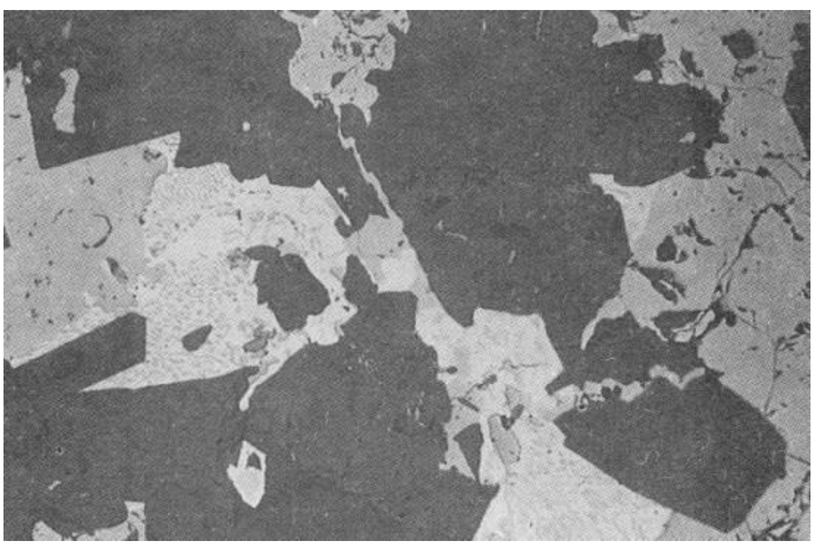

Figure 19. The solid solution separation texture of tellurides (white base) and chalcopyrite (a light grey worm-like mineral with unobvious protrusions), and the metasomatic texture in the contact metasomatic zone between tellurides (white base) and pyrrhotite (gray white). Black is carbonate mineral (thin section (-) ×200)

Structure

The main ore structures are as follows:

Massive: Dense massive ore is the most important structural type in the deposit, and is often composed of coarse-grained lamellar tetradymite as well as other telluride minerals. This kind of ore is almost entirely composed of telluride minerals mainly tetradymite, with little or no other minerals. It is a type of ore only found in rich ore pockets in the deposit.

Vein and/or veinlet: The main manifestations are that tellurium ore bodies intersect in the form of veins or veinlets, cutting the pyrrhotite veins produced in the early stage (Figs. 8, 10, 12 and 18-20).

Stockwork: A stockwork is a complex system of structurally controlled or randomly oriented veins, veinlets and/or stringer zones, which is common in various ore deposits[50]. Telluride veins/veinlets intersect, divide, and surround pyrrhotite in a fine network form or stringer, forming a characteristic stockwork vein structure (Figs. 8, 10, 12 and 18-20).

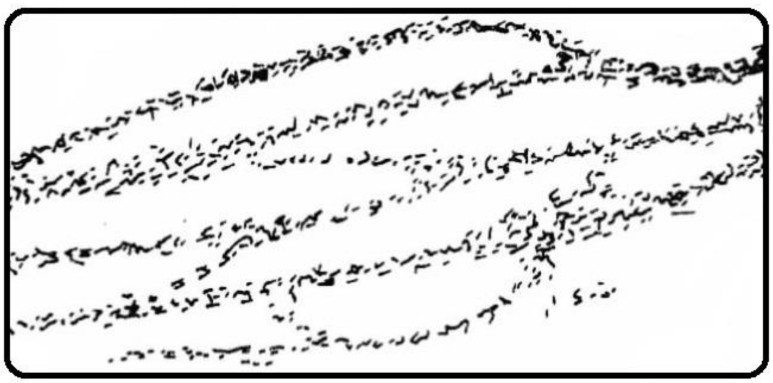

Figure 20. Sketch of telluride stockworks in pyrrhotite in #I-1 ore body

(The scale is the same as Fig. 10)

Dissemination: Tellurium minerals are distributed in pyrrhotite, dolomite, quartz and potassium feldspar veins/veinlets in disseminated, scattered, speckled or patchy forms.

Brecciated: Telluride veins often intersect, divide and develop around pyrrhotite and/or host rock breccia, forming breccia-like structures (Figs. 8-10, 12, 17 and 19).

In addition, giant pentagonal dodecahedral pyrite single crystals are commonly found in pyrrhotite veins, forming a bird's-eye-like structure (Fig. 14).

9.3 Ore type

According to the ore structures, the ores in this deposit can be divided into massive, veinlet-stockwork, and disseminated types. Among them, massive ores account for the largest proportion and are the most important, followed by disseminated ores. The above-mentioned major types of ores can be further divided into several subcategories according to their respective mineral compositions (Table 5).

Table 5. Ore type in the Dashuigou tellurium deposit

Ore type	Ore sub-type	Representative ore body
Massive	Telluride (>85%)-dolomite (<10%)	# I-1, 2, 5, 9, and 10
	Telluride (>85%)-sulfide	# I-1, 2, 4, 5, 7, 8, 9, and 10
Veinlet-stockwork	Telluride (50%-85%)-dolomite (10%-40%)	All of the ore bodies
	Telluride (50%-85%)-sulfide (10%-40%)	All ore bodies except # I-3
	Telluride (50%-85%)-quartz (10%-40%)	Individual ore bodies
Disseminated	Dolomite (>40%)-telluride (<50%)	# I-3
	Pyrrhotite (±pyrite) (>40%)-telluride (<50	All ore bodies except # I-3
	Quartz (±mica) (>40%)-telluride (<50%)	This type of ore is less

Tellurium ore types vary in different ore bodies. In terms of mineral composition alone, dolomite-telluride ore is the most numerous in the deposit.

9.4 Ore composition

The quantitative chemical analysis of the ore through the random chip sampling method shows that the ore of the Dashuigou tellurium deposit contains tellurium between 0.01%-34.58% (Table 6). Previously, Cao et al. concluded that the tellurium ore grade of the deposit is 0.01%-30.63%[45].

Generally speaking, copper and other ores containing 0.002% or more of associated tellurium are valuable. In other words, the minimum recoverable grade of tellurium ore is 0.002%[4-7 & 28].

9.5 Ore property

The ores in this deposit are all deeply buried and have not been exposed to the surface by erosion and thus have not has not suffered any weathering. In other words, the ore in the mining area maintains the state of the original sulfide ore and has not been transformed by oxidation.

This single ore property greatly simplifies the ore processing technology process, thereby greatly saving investment and reducing related expenditures. This is a more positive and economical aspect of developing the deposit.

Table 6. Chemical compositions of the ores in Dashuigou tellurium deposit

	Sample #		SHM-01	SHM-02	SHM-03	SHM-04	SHM-05
Chemical coposition	SiO_2	%	28.60	0.06	0.90	0.62	0.19
	Al_2O_3		23.08	0.32	0.57	0.05	0.15
	Fe_2O_3		18.90	81.62	53.71	3.36	6.56
	CaO		0.67	0.01	10.30	0.05	10.90
	MgO		5.00	0.03	4.72	0.01	4.73
	TiO_2		0.51	0.06	0.06	0.03	0.04
	P_2O_5		0.95	0.21	0.31	0.22	0.21
	MnO		0.04	0.01	0.30	0.01	0.87
	K_2O		0.01	0.00	0.05	<0.001	0.02
	Na_2O		0.55	0.04	0.07	0.00	0.02
	S		5.47	16.41	19.92	4.59	3.15
	H_2S		3.55	1.45	0.37	0.39	0.38
	CO_2		1.35	0.09	17.10	0.19	17.90
	Bi		0.11	<.001	0.12	57.20	35.40
	Te	$\times 10^{-6}$	586	100	656	345800	216600
	Se		<10	18	34	110	100
	F		355	30	20	5	45
	Cl		1.5×10^2	778	620	28	102
	Cu		428	2180	1140	88	237
	Pb		184	16	18	332	206
	Zn		720	-	-	288	25
	B		8600	<1	<1	<1	<1
	Au		0	0	0	2	77
	Au		2	0	1	260	148

10 Paragenetic stage and mineral sequence

Based on the mutually crosscutting relationships of various veins/veinlets in the deposit, including those of pyrrhotite, chalcopyrite, tetradymite, tsumoite, dolomite and quartz, plus related research on ore structure and structure between both gangue and ore minerals under the microscope, two mineralization stages and five sub-stages in the deposit have been confirmed[4,7, 27-28 & 43-44].

10.1 Pyritic stage (177.7~165.1 m.a.)

Including the following three sub-stages as well as mineral sequence (from early to late):

Carbonate sub-stage: A large quantity of iron-dolomite, quartz and lesser calcite veins/veinlets occurred within this stage, which are broken brown and/or yellowish brown coarse-grained due to iron staining (Figs. 8, 10, 12, 15-16, and 18-19). Decrepitation temperatures of the fluid inclusions in the dolomite of this sub-stage are 337.7-397 °C.

Pyrrhotite sub-stage: The largest quantity of pyrrhotite formed during this stage. Some coarse to very coarse-grained pentagonal pyrite can be seen in the anhedral crystals of pyrrhotite (Figs. 8-10, 12, 14, and 17-19). Decrepitation temperatures of the fluid inclusions in both the pyrrhotite and pyrite of this stage are 366.0-406.0 °C.

Chalcopyrite sub-stage: Chalcopyrite veinlets formed within this stage, filling in fractures of pyrrhotite and/or crosscutting pyrrhotite. Part of the chalcopyrite is within telluride minerals in the vermicular form (Fig. 19). Decrepitation temperatures of the fluid inclusions in the chalcopyrite are 298.0-363.0 °C.

10.2 Tellurium stage (91.71~80.19 m.a.)

Including the following two sub-stages as well as mineral sequence (from early to late)
Tetradymite sub-stage: Large quantities of massive/semi-massive tetradymite veins/veinlets formed during this sub-stage, associated with clean, milky-white quartz, dolomite, calcite, muscovite/sericite, native gold and so on (Figs. 8, 10, 12, and 17-20). Decrepitation temperatures of the fluid inclusions in the tetradymite are 186.0-255.0 °C.
Tsumoite sub-stage: There is no doubt that the tsumoite was formed later than the tetradymite. Observation under the microscope seems to indicate that tsumoite is formed by the replacement of pyrrhotite by tetradymite, but this is not necessarily the case. Tsumoite and chalcopyrite together consist of emulsion droplets and/or vermicular immixing of solid solution texture at the contacts between tetradymite and pyrrhotite (Figs.12 and 17-19). The uniform temperature of the fluid inclusions in the quartz associated with the tsumoite indicates that the ore-forming temperature in this sub-stage is 180.0-258.8 °C.

11 Reserve and resource

In view of different understandings of the degree of geological engineering control, estimates of tellurium reserves and resources in this deposit vary greatly, and there is actually no very precise data. Based on relevant previous research data, the proven reserves of tellurium in the Dashuigou tellurium deposit range from 72 to 120 metric tons, and the prospective resources are 300 metric tons[4].

Based on the above relevant reserve data, we will use the relevant methods proposed by Laznicka[51] to define the scale of Dashuigou independent tellurium deposit.

If we use the crustal abundance or Clark value of tellurium published by Li Tong in 1976 and 1990[1-2], which is 6×10^{-10}, we can conclude that the tonnage accumulation indices of Dashuigou tellurium deposit are 1.2×10^{11}, 2.0×10^{11}, and 5.0×10^{11}, all exceeding 1.0×10^{11}, indicating that the deposit is a super large independent tellurium deposit. If the average abundance or Clark value of tellurium in the crust announced by Li etc. in 1994[3] is used, which is $2 \text{ x } 10^{-8}$, a similar conclusion can be drawn; that is, the deposit is a super-large independent tellurium deposit.

12 Discussion

Produced at the NE end of the dome, the deposit’s entire Te ore bodies are limited to the schist/phyllite/slate in the middle of the dome. Both the early pyrrhotite veins and late tellurium ore veins filled in a group of fissures with shear properties. The later tellurium veins or veinlets filled in the compressive shear fractures developed in the early pyrrhotite veins.

The hanging and foot walls of the #I-5 ore body indicate that the contact between schist and banded marble in the study area is one of the favorable ore-hosting spaces and is naturally one of the good prospecting targets in the study area.

Both pyrrhotite and telluride veins have very clear contact with the altered host rocks and/or between the two different veins themselves. Meanwhile, the altered zones are very narrow and non-zoned. This may suggest that the deposit was formed through slurry penetration.

Scale-like muscovite and/or sericite in late quartz veins, or those symbiotic with late dolomite in the form of veinlets in host rocks close to the tellurium mineralization constitute another important prospecting indicator for potential tellurium deposits in the region.

Field geological observations show that the geological times of pyritic veins, tellurium veins and their associated alteration types are far apart, not products of the same mineralization period or geological event. Pyrrhotite is ubiquitous in the study area, whereas tellurium mineralization is much more localized. In other words, there is no necessary connection between tellurium mineralization and pyritic mineralization. Geological dating proves this.

The most favorable mineralization zone is where muscovitization/sericitization, dolomitization and silicification are superimposed and compounded.

In short, the wall rock alteration in the mining area is a product of different geological periods. The wall rock alteration related to the pyrrhotite veins is a product of the early Yanshan orogeny, while that related to the tellurium veins is a product of the late Yanshan orogeny.

The research area has a unique geotectonic background and geological conditions, with a considerable number of favorable channels/fault zones for mantle material to rise. In view of this, numerous rare and dispersed element deposits, including more tellurium deposits, will be discovered in the area in the near future.

The texture and structure of ores reflect the characteristics, similarities and differences of the mineralization period, mineralization stages and mineral generation sequence. As a result, ore texture and structure are one of the important foundations for dividing the mineralization stage, sub-stage, and mineral sequence of a mineral deposit.

According to Table 6, it can be seen that Te has an obvious positive correlation with Bi and Ag, and generally has the same growth and decline trend as Se, Au and Cu. In this regard, we can roughly understand that Te, the corresponding minerals of Bi and Ag are products of the same paragenetic stage, and the corresponding minerals of Se, Au and Cu are most likely products of the same mineralization period. This is consistent with the results observed under the microscope; that is, tetradymite, chalcopyrite, and Au-Ag series of minerals are all products of the late Yanshan orogeny.

The ore grade of Dashuigou independent tellurium deposit has far exceeded the minable grade of associated tellurium ore by 5.00 to 1.73×10^4 times, and its highest grade is even more than 1.73×10^4 times.

In terms of tellurium alone, the economic value of the Dashuigou deposit is self-evident. Fortunately, the ore also contains high grade of beneficial elements such as Bi, Au and Ag, and thus has high comprehensive utilization value (Table 6).

All ores in the deposit are primary sulfide without oxidation transformation.

Based on the cutting and interpenetrating relationships between mineral veins in different geological times and the mineral generation sequence, supplemented by K-Ar isotope dating, we concluded that this deposit’s formation was caused by two paragenetic stages consisting of a total of 5 mineralization sub-stages.

13 Conclusions

Based on the unique geotectonic and geological setting in the study area, especially the favorable passage for mantle material to rise, numerous rare and dispersed element deposits, including more brand new independent tellurium deposits, will be discovered in the near future in the area.

Although nearly 40 minerals have been discovered in the ore of the deposit, it is expected that with the deepening and refinement of ore mineral research, it is possible to discover some unknown new minerals in the near future, considering the special geotectonic background and geological setting of the deposit in the study area.

The tonnage accumulation indices of the Dashuigou independent tellurium deposit indicate that it is a super-large independent tellurium deposit in the world.

Acknowledgements Support for this study was received from Orient Resources Ltd. in BC, Canada; Wuhan Institute of Technology; and College of Earth Sciences, Jilin University in China. It must be pointed out that the scanning electron microscope pictures in this article; namely Figs. 12 and 18, were completed and generously provided by Ms. Jordan Roberts in the relevant laboratory of the University of British Columbia in Canada. The authors of this article express sincere gratitude to her for her hard work and selfless dedication. The chemical analyses included in this article were carried out in the labs of the Chinese Academy of Geological Sciences in Beijing, while the K-Ar dating was completed by relevant laboratory of the Institute of Geology of the State Seismological Administration of China in Beijing.

Author contributions JZ Yin proposed and contributed to the whole research, interpretation, and writing of the paper. All other authors including HY Yin, YH Cao, SP Xiang, and HY Shi contributed to the data collection and compilation of this paper. All authors prepared and reviewed the manuscript and approved the final version of the manuscript.

Data availability statement The data that support the findings of this study is available from the authors upon reasonable request.

Declarations The authors declare that they have no conflict of interest.

14 References

1. Li, T. 1976. Abundance of chemical elements in the Earth. *Geochemistry*, 3**:** 167-174 (**in Chinese**).

2. Li, T & Ni, SB. 1990. *Abundance of chemical elements in the Earth and crust*. Beijing: Geological Publishing House, 136pp (**in Chinese**).

3. Li, T: Yuan, HY; Wu, SX & Cheng, XF. 1999. Regional abundance of chemical elements of crust bodies in China. *Geotectonica et Metallogenia*, 23(2): 101-107 (**in Chinese with English abstract**).

4. Yin, JZ. 1996. *On the paragenetic model and mineralizing mechanism of the Dashuigou independent tellurium deposit in Shimian County, Sichuan Province, China-the only independent tellurium deposit in the world.* Chongqing: Chongqing Publishing House, 190 pp (**in Chinese with English abstract**).

5. Yin, JZ; Chen, YC & Zhou, JX. 1995e. Introduction of tellurium resources in the world. *Journal of Hebei College of Geology* 18(4): 348-354 (**in Chinese with English abstract**).

6. Cheng, ZY; Zhu, XM and Zeng,Y. 2020. Current status of tellurium extraction and utilization. *Mineral Protection and Utilization*, 40(5): 76-89 (**in Chinese**).

7. Yin, JZ. & Shi, HY. 2020a. Mineralogy and stable isotopes of tetradymite from the Dashuigou tellurium deposit, Tibet Plateau, Southwest China. *Scientific Reports*, 10: 4634 | hppts://doi.org/10.1038/s41598-020-61581-3.

8. Cao, ZM; Wen, CQ & Li, BH. 1995. Genesis of the Dashuigou tellurium deposit in Sichuan Province of China. *Science China (B)*, 25(6): 647-654 (**in Chinese with English abstract**).

9. Chen, PR; Lu, JJ; Wang, RC; Xu, SJ & Chen, XM. 1998. Study on the fluid inclusions of the Dashuigou independent tellurium deposit in Shimian County, Sichuan Province, China. *Mineral Deposit*, 17 (special issue): 1011-1014 (**in Chinese with English abstract**).

10. Chen, YC; Mao, JW; Luo, YN; Wei, JX & Cao, ZM. 1996. *Geology and Geochemistry of the Dashuigou tellurium (gold) deposit in Western Sichuan, China*. Beijing: Atomic Energy Press, 146pp (**in Chinese with English abstract**).

11. Chen, YC; Mao, JW; Zhou, JX & Yin JZ. 1993. Dashuigou tellurium gold deposit in Shimian County, Sichuan Province - the world's first independent tellurium deposit mainly composed of tellurium. In: *Proceedings of the Fifth National Conference on Mineral Deposits*. Beijing: Geological Publishing House, 437-439 (**in Chinese**).

12. Li, BH; Cao, ZM; Jin JF & Wen, CQ. 1999. Physicochemical conditions of the tellurium deposit in Dashuigou, China. *Scientia Geologica Sinica*, 34(4): 463-472 (**in Chinese with English abstract**).

13. Li, BH; Cao, ZM & Wen, CQ. 2000. Fluid inclusion type and geological characteristics of the Dashuigou tellurium deposit in Sichuan Province, China. *Bulletin of Mineralogy, Petrology and Geochemistry*, 4**:** 346-347 (**in Chinese with English abstract**).

14. Liu, AP; Zhong, ZC & Tang, JW. 1996. Geochemical characteristics of the Dashuigou tellurium deposit in Sichuan Province of China. *Geochemistry*, 25(4): 365-371 (**in Chinese with English abstract**).

15. Luo, YN & Cao, ZM. 1994. The world's first independent tellurium deposit was discovered in Sichuan Province. *China Geology*, (2): 27-28 (**in Chinese with English abstract**).

16. Luo, YN; Cao, ZM & Wen, CQ. 1996. *Geology of the Dashuigou independent tellurium deposit*. Chengdu: Southwest Communication University Publishing House, 30-45 (**in Chinese with English abstract**).

17. Luo, YN; Fu, DM & Zhou, SD. 1994. Genesis of the Dashuigou tellurium deposit in Sichuan Province of China. *Bulletin of Sichuan Geology*, 14(2): 101-110 (**in Chinese with English abstract**).

18. Luo, YN; Fu, DM; Zhou, SD; Cao ZM & Li DH. 1994. Geology and genesis of the Dashuigou tellurium deposit in Shimian County, Sichuan Province. *Sichuan Geological Journal*, 14(2): 1-10 (**in Chinese with English abstract**).

19. Mao, JW; Wei, JX & Yang, BC. 1995. A preliminary study on the genesis of the Dashuigou tellurium deposit in Shimian County, Sichuan Province, China. *Bulletin of Mineralogy, Petrology and Geochemistry*, (1): 23-24 (**in Chinese with English abstract**).

20. Shen, WZ; Xu, XJ & Wang, RC. 1997. Origin of the fluid inclusions of the Dashuigou tellurium deposit in Sichuan Province, China- hydrogen and oxygen isotope evidence. *Journal of Nanjing University (Natural Sciences)* 33, special issue: 77-83 (**in Chinese with English abstract**).

21. Wang, RC; Lu, JJ & Chen, XM. 2000. Genesis of the Dashuigou tellurium deposit in Sichuan Province, China. *Bulletin of Mineralogy, Petrology and Geochemistry*, 4: 348~349 (**in Chinese with English abstract**).

22. Wang, RC; Shen, WZ; Xu, XJ; Lu, JJ; Chen, XM; Luo, YN & Cao, ZM. 1995. Isotopic geology of the Dashuigou tellurium deposit in Sichuan Province, China. *Journal of Nanjing University (Natural Sciences)*, 31(4): 617-624 (**in Chinese with English abstract**).

23. Wei, JX & Mao, JW. 1998. Characteristics of ore-forming fluids and their mantle-derived properties in the Dashuigou tellurium deposit. *Deposit geology*, 17: 1091-1094 (**in Chinese with English abstract**).

24. Xu, SJ; Shen, WZ & Wang, RC. 1998. Zircon-U-Pb dating of ore-bearing amphibolites from the Dashuigou tellurium deposit. *Science Bulletin*, 43(8): 883-885.

25. Yin, JZ. 1996a. The paragenetic model and mineralizing mechanism of the Dashuigou independent tellurium deposit in Shimian County, Sichuan - the first and only independent tellurium deposit in the world. *Acta Geoscientia Sinica*, special issue: 93-97.

26. Yin, JZ. & Shi, HY. 2019b. Nano effect mineralization of rare elements--taking the Dashuigou tellurium deposit, Tibet Plateau, Southwest China as the example. *Academia Journal of Scientific Research*, 7(11): 635-642. DOI: 10.15413/ajsr.2019.0902.

27. Yin, JZ. & Shi, HY. 2021b. Fluid inclusions and metallogenic conditions of the Dashuigou tellurium deposit, Tibet Plateau, southwest China. *Geology, Earth & Marine Sciences*, 3(3): 1–15.DOI: 10.31038/GEMS.2021331.

28. Yin, JZ; Xiang, SP; Chao, YH; Yin, HY & Shi, HY. 2022d. Petrochemical eigenvalues and diagrams for the identification of metamorphic rocks' protolith, taking the host rocks of Dashuigou tellurium deposit in China as an example. *Acta Geochimica*. DOI: 10.1007/s11631-022-00583-6.

29. Xu, ZQ; Hou LW; Wang, ZX; Fu XF & Huang MH. 1992. *The orogenic process of the Songpan-Ganzi orogenic belt in China*. Beijing: Geological Publishing House, 190pp (**in Chinese with English abstract**).

30. Huang, H; Huyskens, M.H & Yin, QZ. 2022b. Eruptive tempo of Emeishan large igneous province, southwestern China and northern Vietnam: relations to biotic crises and paleoclimate changes around the Guadalupian-Lopingian boundary. *Geology*, https://doi.org/10.1130/G50183.1.

31. Shen, FQ. 1985. Trace elements geochemistry of igneous rocks assemblage in Panzhihua-Xichang rift. *Scientific Sinica*, (9): 844-855.

32. Yin, JZ; Zhou, JX & Yang, BC. 1994n. Geological characteristics of the Dashuigou tellurium deposit in Sichuan Province, China. *Earth Science Frontiers*, 1(4): 241-243 (**in Chinese with English abstract**).

33. Chen, YC; Yin, JZ & Zhou, JX. 1994b. Geology of the Dashuigou independent tellurium deposit of Sichuan Province. *Acta Geoscientia Sinica*, 29(2): 165-167 (**in Chinese with English abstract**).

34. Chen, YC; Yin, JZ & Zhou, JX. 1994a. The first and only independent tellurium ore deposit in Dashuigou, Shimian County, Sichuan Province, China. *Sci. Geol. Sinica*, 3(1): 109-113 (**in Chinese with English abstract**).

35. Mao, JW; Chen, YC & Zhou, JX. 1995. Geology, mineralogy, petrology, and geochemistry of the Dashuigou tellurium deposit in Shimian County, Sichuan Province, China. *Acta Geosciences*, 2(3): 276-290 (**in Chinese with English abstract**).

36. Yin, JZ; Chen, YC & Zhou, JX. 1996b. Geology and geochemistry of host rocks of the Dashuigou independent tellurium deposit in Sichuan Province, China. *Journal of Changchun University of Earth Sciences* 26(3): 322-326 (**in Chinese with English abstract**).

37. Yin, JZ; Xiang, SP; Yin, HY; Shi, HY; & Chao, YH. 2023. Origin of the Dashuigou independent tellurium deposit at the southeastern Qinghai-Tibet plateau: based on the abundances of trace elements in the country rocks. *Advances in Geological and Geotechnical Engineering Research*. 5(4): 41-55. DOI: https://doi.org/10.30564/agger.v5i4.5967.

38. Yin, JZ; Chen, YC and Zhou, JX. 1995d. Original rock of the host rock of the Dashuigou independent tellurium deposit in Sichuan Province, China. *Bulletin of Mineralogy, Petrology and Geochemistry*, (2): 114-115 (**in Chinese with English abstract**).

39. Yin, JZ; Chen, YC & Zhou, JX. 1996d. Geology and geochemistry of altered rocks of the Dashuigou independent tellurium deposit in Sichuan Province, China. *Journal of Xi'an College of Geology*, 18(4): 19-25 (**in Chinese with English abstract**).

40. Yin, JZ; Zhou, JX & Yang, BC. 1994g. Rock-forming minerals and ore-forming minerals of the Dashuigou tellurium ore deposit unique in the world - A preliminary study. *Sci. Geol. Sinica*, 3(2): 197-210.

41. Yin, JZ; Chen YC & Zhou, JX. 1994k. Mineralogical research of the Dashuigou independent tellurium deposit in Sichuan Province, China. *Bulletin of Mineralogy, Petrology and Geochemistry*, (3): 153-155 (**in Chinese with English abstract**).

42. Yin, JZ; He, DS; Yin, YH; Shi, H & Xiang, SP. 2022. On ore from the Dashuigou tellurium deposit, Tibet plateau, southwest China. *European Journal of Applied Sciences*, 10(6): 458-472.

43. Yin, JZ; Chen, YC & Zhou, JX. 1995a. The metallogenic age of the world's first independent tellurium deposit. *Chinese Science Bulletin*, 40: 766-767 (**in Chinese with English abstract**).

44. Yin, JZ; Chen, YC & Zhou, JX. 1995b. K-Ar isotope evidence for age of the first and only independent tellurium deposit. *Chinese Science Bulletin*, 40(22), 1933-1934.

45. Cao, ZM & Luo, YN. 1993. Geological characteristics and material composition of the Shimian Te (Se) deposit in Sichuan Province. In: *Proceedings of the Fifth National Conference on Mineral Deposits*. Beijing: Geological Publishing House, 476-476 (**in Chinese**).

46. Mao, JW; Chen, YC; Yang, BC; Lei, YF & Zhou, JX. 1995. Study on tetradymite in Dashuigou tellurium polymetallic deposit, Shimian County, Sichuan Province, China. *Geological Science*, 30(1): 47-52 (**in Chinese with English abstract**).

47. Wang, RC; Chen XM & Xu, SJ. 1996. Complex exsolution of tellurium minerals in the Dashuigou tellurium deposit. *Science Bulletin*, 41(10): 920-922.

48. Cao, ZM & Luo, YN. 1994. Mineral sequence and ore genesis of the Sichuan telluride lode deposit in China. In: *New Research Progresses of the Mineralogy, Petrology and Geochemistry in China*. Lanzhou: Lanzhou University Publishing House, 476-478 (**in Chinese**).

49. Department of Geology, Nanjing University. 1987. Crystallography and Mineralogy. Beijing. Geological Publishing House, 659pp.

50. Ash, C & Alldrick, D. Vein, Breccia, and Stockwork. www.empr.gov.bc.ca/. British Columbia Geological Survey. Retrieved 1 November, 2013.

51. Laznicka, P. 1989. *Giant Metallic Deposits: Future Sources of Industrial Metals*. Springer, 2nd edition, 961pp.